

AC: We would like to thank the reviewer for their insightful comments and suggestions, which we believe have significantly improved the quality of this manuscript as well as our research.

AC: The following document is organized in two sections. In the first section we have addressed reviewer #1 comments and in the second section we have addressed reviewer #2 comments. At the end of section 2, reviewers can find the References section.

AC: We would also like to note to the reviewer that we have accepted the suggestion of the other reviewer to use the Guzinsky et al. (2013) method based on the EVI and NDVI to estimate the f_G . According to Fisher et al. 2008, f_G is defined by $FAPAR / FIPAR$ where FAPAR is the fraction of PAR absorbed by green vegetation cover and FIPAR the fraction of PAR intercepted by total vegetation cover. Due to a lack of FAPAR observations, we estimated f_G using only FIPAR as suggested by Anser (1998) and as the results show this might have caused an overestimation of f_G at the beginning and at the end of the growing season contributing to model-measurement disagreement. Although this was not a major point according to the reviewer, we have re-run the model using Guzinsky et al. (2013) approach to estimate f_G . The new results yielded better model agreement, although it does not provide reliable f_G values at the end of the season (mainly in September) and further research needs to address this issue.

Reviewer #1 comments

RC_1: p9, l24–27 The method to estimate f_G is not clear to me. How do you estimate the fraction of absorbed PAR by the green vegetation? Is it equal to PAR incoming - PARreflected in your model? This would also include PAR absorption by bare soil, dead plant material, mosses and other elements. Guzinski et al. (2013) actually suggests to use a different method, based on NDVI and EVI (as you mention on page 14). Do you have another reference that actually recommends the PAR ratio method?

AC_1: We would also like to note to the reviewer that we have accepted his/her suggestion to use the Guzinsky et al. (2013) method based on the EVI and NDVI to estimate the f_G . According to Fisher et al. 2008, f_G is defined by $FAPAR / FIPAR$ where FAPAR is the fraction of PAR absorbed by green vegetation cover and FIPAR the fraction of PAR intercepted by total vegetation cover. Due to a lack of FAPAR observations, we estimated f_G using only FIPAR as suggested by Anser (1998) and as the results show this might have caused an overestimation of f_G at the beginning and at the end of the growing season contributing to model-measurement disagreement. Although this was not a major point according to the reviewer, we have re-run the model using Guzinski et al. (2013) approach to estimate f_G . The new results yield a better model agreement, although it does not provide reliable f_G values at the end of the season (mainly in September).

RC_2: 1. The authors stress the point that a remote-sensing based model can be applied at the larger scale (Title, Abstract p. 1, l. 17, 24, 26; Motivation p. 3, l. 1–12; Conclusions p. 15, l. 8–10). However, it seems that (except for the LAI, which is a minor point of the study) this was not done (p. 11, l. 23–24). This is a little bit disappointing after reading pages 1–3. Therefore I would suggest to force the model with satellite data only and compare the results. If this is beyond the scope of the paper, the authors should adjust the motivation statements.

This paper is focused on the local application with the tower micrometeorological and flux measurements representing local conditions in order to more reliably evaluate and refine the TSEB model for regional application to the Arctic tundra. As we stated in the conclusion section we will extend this research to regional scales using a TSEB-based model refined to be robust for the Arctic tundra using satellite inputs. To better clarify this objective, we have added text to the introduction motivating the need for localized testing in preparation for improvement of a regional satellite based energy balance model.

RC_2: 2. Section 2 is quite long given that the model description is published already. P4 l20 – p5 l12 could be omitted or moved to an appendix as the resistance terms and the sensible heat flux parameterisation are not discussed further in the manuscript. In this case, you could mention after Equation 11 that H_s is calculated as a function of the difference between canopy air temperature and soil temperature and of the soil resistance.

AC_2: Given questions raised by the second reviewer about the model formulation, we decided to retain the discussion of the TSEB formulations needed to understand the resulting refinements required to obtain good results (see discussions in sections 3 and 6).

RC_3: 3.1. You show two different approaches for estimating c_G (Section 3.2). In both approaches you fit some parameters. However, if I understand it correctly, you use different data for fitting. On what data did you fit the parameters of the first method (p7, 123–24)? Why did you not use the same approach as for the second method, where you split the data set into a calibration and a validation subset? Are the data of all stations combined in a single data set? Do you take an equal amount of data points per station? Are the parameters fitted separately for month? Please describe the fitting approach in more detail in Section 3.2.

AC_3: We have improved section 3.2, 4.2 and Tables 3 and 4 to clarify these points. The Kustas et al. (1998) and Santanello and Friedl (2003) methods were evaluated against the same dataset used to evaluate all fluxes that had restrictions for balance closure, among others (see section 4.2). To fit and test the new c_{TG} approach, data from the previous dataset with no restriction of balance closure and from 4 to 21 hours local solar time was used. Coefficients A, B and S were derived using 60% of all available data aggregated in 30 min timesteps for the whole summer period and the remaining 40% of the data were reserved for model testing. Table 4 shows the amount of data points per station (n) to derive model coefficients and test the c_{TG} approach. To calibrate the c_{TG} , for the Tussock and Heath flux towers n is similar (around 10 000) while for the Fen tower, less data were available (n ~8 000).

RC_4: 3.2. Would it be possible to use a proxy such as soil moisture to improve the fit?

AC_4: Soil heat flux plate measurements were corrected to account for soil heat storage using soil moisture from the water content reflectometers. This has been added to the text.

RC_5: 3.3. Although you mention that soil type and properties are important, none of your methods takes it into account.

AC_5: We agree with the reviewer that soil type and properties are important to model G. In the original TSEB formulation, a simple approach based on the relationship between G and R_{NS} was used (Eq. 13). This approach has less complexity and requires no soil texture and moisture information, which, unfortunately, is not routinely available over large areas. For continental-to-global applications of the TSEB, we are indeed finding that variations in the main parameters of the G formulation are required – for example over rock or desert sands. However, the modifications derived here help to better capture thermal characteristics of the tundra substrate.

RC_6: 4. In Section 3.3 you describe that you use two different Priestley-Taylor coefficients.

Did you consider varying them with soil moisture or LAI? Are they valid for the whole Arctic, or only locally?

AC_6: The initial values of the Priestley-Taylor coefficients (PTC) we used in this paper were the originally proposed value of 1.26 for application of TSEB and a value of 0.92 averaged from

the references found in the literature focused on Arctic tundra. As a starting point for the model we consider this range in PTC applicable for Arctic vegetation.

AC_6: In addition, to clarify how TSEB can adjust PTC for moisture conditions, the following paragraph has been added in section 2: “Under stress conditions, TSEB iteratively reduces α_{PTC} from its initial value. The TSEB model requires both a solution to the radiative temperature partitioning (Eq. 2) and the energy balance (Eqs. 6 and 7), with physically plausible model solutions for soil and vegetation temperatures and fluxes. Non-physical solutions, such as daytime condensation at the soil surface (i.e., $LE_S < 0$), can be obtained under conditions of moisture deficiency. This happens because LE_C is overestimated in these cases by the Priestley–Taylor parameterization, which describes potential transpiration. The higher LE_C leads to a cooler T_C and T_S must be accordingly larger to satisfy Eq. (7). This drives H_S high, and the residual LE_S from Eq. (11) goes negative. If this condition is encountered by the TSEB scheme, α_{PTC} is iteratively reduced until $LE_S \sim 0$ (expected for a dry soil surface). However there are instances where the vegetation is not transpiring at the potential rate but is not stressed due to its adaption to water and climate conditions (Agam et al., 2010) or the fact that not all the vegetation is green or actively transpiring (Guzinski et al., 2013).”

RC_7: 5. Figure 2 does not demonstrate a relationship between TRAD and G, it merely shows that both variables exhibit a diel cycle (p11, l11–12 & p15, l1–2). Can you please provide more details on the expected relationship? I find that this is an important point as one of your main conclusions is that the approach using TRAD is better than using RN. If I understand your reasoning correctly, you assume that the relationship between TRAD and G holds for different vegetation types, times of the growing season and weather conditions. This point needs to be discussed in more detail. For example, a recent study by Juszak et al. (2016) showed that two different vegetation types with close to identical top soil temperatures differed in G by a factor of 2. It would be great if you showed evidence for this relationship under different conditions. I would at least expect to see scatterplots of TRAD and G as compared to RN and G and correlation coefficients. Of course you can use shifted time series to account for the time lack.

RC_7: Figure 2 The temperature is not in Kelvin. I do not think it makes sense to take the mean of all available data as the station with most data will contribute more and biases can occur, for example if the coldest station on average starts measuring later during the year. I would prefer one plot per station, or a completely different graph (as explained above).

AC_7: The axis title has been corrected. The relationship between TRAD and G and the definition of the new coefficient c_{GT} has been explained in section 3.2 in which G is computed using Eq. 18. This method uses a phase shift proposed by Santanello and Friedl (2003) and is supported by the measurements illustrated in Figure 2. Figure 2 was only meant to show this phase shift and text in p11, l11–12 has been changed accordingly. Figure 3 and Table 4 show the behaviour of the new coefficient c_{GT} derived from the TRAD-G relationship on a per station basis.

RC_7: 6. The results and discussion in Section 6 are for all stations combined. However, it would be interesting to read about the different (or similar) accuracies at the different vegetation types. This is particularly relevant if you want to conclude on vegetation

dynamics and vegetation change (p14, l20–22). Figures 4 and 5 also reveal differences between the stations. For example LE is strongly overestimated at the tussock site. Why?

AC_7: Unfortunately, without detailed ground measurements to verify the assumed TSEB vegetation inputs (such as LAI), it is hard to identify any single factor that may have been a major cause for model-measurement disagreement, but overall the TSEB performance is considered satisfactory for all sites evaluated in this paper.

RC_8: 7. Why do you discuss the accuracy of RN (p12, l8–16; p14, l6–11, l24, l30–31, most figures and tables) and not of the incoming longwave radiation alone? If you use the shortwave radiation budget and outgoing longwave radiation from measurements and just compute the incoming longwave radiation in your model, it would be surprising if you found a substantial difference in RN. Did you use any of the remote sensing products (p12, l15–16) to justify your conclusion that 'this methodology scheme can be used to obtain reliable estimates of RN'?

AC_8: Downwelling longwave radiation results were discussed at the beginning of section 6.2 before discussing RN results.

AC_8: We have not used remote sensing products to justify this conclusion. This sentence has been rewritten accordingly.

RC_9: 8. All Figure legends, scale bars and axis labels are far too small. Please increase the font size to about the same as the figure caption. Please also avoid to rotate the figures (in figures 6,8,9) and the axis labels.

AC_9: Figure legends, scale bars and axis labels have been increased.

AC_9: Figures 6, 8 and 9 have been re-rotated.

RC_10: p1, l19 What is unique about tundra conditions?

AC_10: "Unique" was misplaced. It was supposed to be written before "parameterizations". In any case it has been removed from the text to avoid leading to misinterpretations.

RC_11: p1, l24–25, Section 2 How did you test the usefulness of the MODIS LAI? Maybe it would be helpful to compare the results of the three towers concerning the different LAI. Also, did you test if the model is sensitive to LAI variations? Which fluxes are influenced by LAI in the model?

AC_11: Unfortunately, we do not have LAI field measurement, thus, MODIS LAI usefulness was tested indirectly by means of the evaluation of the surface energy fluxes. The model is sensitive to LAI, since the radiation and temperature partitioning are affected by the LAI/fractional cover as well as the wind speed at the soil surface and LEc via the PT parameterization for the Rnc (Timmermans et al., 2007).

RC_12: p9, l21–22 Other comprehensive LAI data from close-by can be used as reference,

e.g. Shaver and Chapin (1991); Shippert et al. (1995); Williams et al. (2001); Walker et al. (2003); Williams et al. (2006); Shaver et al. (2007); Sweet et al. (2015). In particular the study of Williams et al. (2006) has many details on different types. I am sure there are even more studies which measured LAI as the Imnavait Watershed and Toolik lake are very well studied.

RC_12: p13, l30 An LAI of 1.7 seems to be quite high for the Imnavait Watershed. Did you compare with other data such as (Shaver and Chapin, 1991; Shippert et al., 1995; Williams et al., 2001; Walker et al., 2003; Williams et al., 2006; Shaver et al., 2007; Sweet et al., 2015)? Which vegetation type had this extreme value?

AC_12: References about reported LAI values in these previous works and alternative methods to estimate LAI in the Arctic tundra have been added.

RC_13: p1, l29 Omitting 'Near-surface or shelter level' would make the starting sentence more catchy.

AC_13: This has been deleted from the text.

RC_14: p2, l2–4 Less references would be enough.

AC_14: We have kept more recent and relevant publications.

RC_15: p2, l15 Do you really mean 'inconsistent', or rather 'sparse'?

AC_15: We meant spatially and temporally inconsistent, and we did not imply that the data is wrong in any sense. We have rewritten the sentence to avoid misinterpretations.

RC_16: p2, l18 What is an 'increase in peak vegetation'? Do you mean vegetation growth / activity / LAI?

AC_16: According to Jia et al., 2003 it is in the “peak vegetation greenness”. The reference was misplaced. This has been changed in the text.

RC_17: p2, l19 Do fires contribute to the greening? Maybe it would make sense to exchange the first two sentences of this paragraph.

AC_17: Sentences have been exchanged in the text.

RC_18: p2, l24–25 As shown in the recent paper by Williamson et al. (2016), the albedo effects of shrubs may not be as clear. Also, wet surfaces and sparsely vegetated water may have an even lower albedo than shrubs (Gamon et al., 2012).

AC_18: We agree with the reviewer that wet surfaces and sparsely vegetated water may have an even lower albedo than shrubs. A reference to the Williamson et al. paper has been added to the paper.

RC_19: p4, l7 Does this mean that the model uses a spherical leaf angle distribution for all vegetation? How do the results change, if an erectophile distribution is used for the graminoid vegetation (fen, tussock tundra)?

AC_19: The assumed leaf angle distribution will affect the radiation divergence through the canopy layer and hence affect the net radiation partitioning between the canopy overstory and the soil/substrate. Without measurements to determine the leaf angle distribution, the default of a spherical leaf angle distribution is a reasonable one, particularly for heterogeneous surfaces having a mixture of vegetation species.

RC_20: eq. 1, 4–12 It is a bit confusing that R can be radiation or resistance, depending on the subscript. Maybe you could use 'r' for the resistance values?

AC_20: “r” has been adopted for resistance and changed in the text.

RC_21: p5, l25 The abbreviation TIR is not explained. Additionally, this paragraph suggests that the satellite data is used for the study. If this is not the case, delete the clause 'when daytime TIR satellite imagery is typically acquired'.

AC_21: we have expanded the TIR abbreviation. This paragraph refers to the original method development in which $c_G=0.3$ was set. However, in order to avoid misinterpretations we have deleted “when daytime thermal satellite imagery is typically acquired” from the paragraph.

RC_22: Section 3.1 Why do you continue using the Brutsaert (1975) formula? Two comparison studies on empirical parametrisations of incoming longwave radiation found that other formulars described the data better, namely the Dilley and O'Brien (1998) clear sky formula and the Unsworth and Monteith (1975) cloud correction (Flerchinger et al., 2009; Juszak and Pellicciotti, 2013).

AC_22: Although there are other sky emissivity parameterizations which might give slightly better estimates of incoming longwave, the error in using Brustaert formulation in TSEB is minor compared to the errors in turbulent flux estimation. In fact from Table 5 in Flerchinger et al (2009) the RMSD from all sites measuring incoming longwave using Brutsaert (1975) is 27.2 W/m² while for Dilley and O'Brien (1998) it is 23.3 W/m². Regarding cloud correction, the Crawford and Duchon method is easier to apply since we do not have the data required for Unsworth and Monteith (1975) method.

RC_23: p7, l5 & p.7, l 25–29 Actually, in Eq. 12, not RN is used but RNS. Please make more clear which variable you use. And if you adjusted the model in case you use RN.

AC_23: This has been corrected in the text.

RC_24: p7, l8–14 Exchange this paragraph with the first paragraph.

AC_24: This has been exchanged in the text.

RC_25: p7, 115–17 Split the sentence in two parts as the 'while' does not follow easily on the first part of the sentence.

AC_25: This has been corrected in the text.

RC_26: p7, 123–24 Why does this sentence not appear in the results section?

AC_26: These are the values from the original model. We have rewritten the sentence to clarify the text.

RC_27: p8, 113 Remove '1.2.1'.

AC_27: This has been removed from the text.

RC_28: p9, 18 Are you sure you have several Dryas species (as indicated by spp)? Also, Dryas is a dwarf shrub species, so it would be more accurate to write '..., other dwarf shrubs, and lichen'.

AC_28: This has been modified in the text accordingly.

RC_29: p9, 111 What do you mean by 'vegetation-based measurements'? Maybe replace the term with 'canopy structure' or 'vegetation properties'.

AC_29: We have changed the section title using “vegetation properties”.

RC_30: p9, 129 Can you explain your choice of 1 for the clumping factor in more detail? What is a 'variable organic layer'?

AC_30: It is not an organic layer, it is a moss layer, and this has been changed in the text. As text says clumping factor was set to 1 based on the knowledge that Arctic tundra has a variable moss layer with little bare ground, thus, almost covering almost 100% of the ground. We used this approach for modelling purposes as we do not have actual data on the ground. However, a value of 1 seems a realistic approach for the study area.

RC_31: p9, 130 Vegetation height and the clumping factor are not variable. Can you estimate the uncertainty you introduce with this assumption?

AC_31: Over the growing season ground measurements indicated little change in vegetation height and density. Prior sensitivity studies (e.g., Zhan et al., 1996) indicate TSEB shows relatively small sensitivity to canopy height and fractional cover, which is related to the vegetation clumping factor.

RC_32: p10, 11–2 The sentence about future work should be moved to the discussion or conclusions.

AC_32: This sentence has been moved to the conclusions section.

RC_33: p10, 112–13 Why do you restrict the modelling to daytime conditions? It would be interesting to also test if the model is able to reproduce values at night. I am aware, that the incoming longwave radiation depends on cloud cover. However, you could interpolate the cloud cover during the night. How did you assess the presence of precipitation?

AC_33: Our testing is focused on daytime conditions for two reasons: First, EC flux observations used for validation are less reliable during night-time due to stable conditions and low wind speeds. Second, for transition to satellite applications, we are primarily interested in evaluating model performance during daytime satellite overpass times. Other techniques are typically used to upscale from the overpass time to daily total fluxes.

RC_34: Section 5 Using five different error estimates does not add additional information as compared to using only three. In your results, you rarely mention MAD and the information of MAPD and RMSE is largely the same. It is not very intuitive that in your notation the mean of e_i is \bar{X} . You could use e_i and \bar{E} or x_i and \bar{X} (and the corresponding notation for o_i and \bar{Y}) instead.

AC_34: We have used five different error estimates to make the results section more comparable to other papers. Although we agree with the reviewer, in the literature you may find some studies in which MAE or MAD are only stated.

AC_34: e_i and o_i notations have been changed in the text.

RC_35: p11, 121 & Table 4 What is this flux subset? Please describe the choice of the subset in the methods.

AC_35: This was clarified in section 4.2 “Model inputs and evaluation dataset” and Tables 3 and 4.

RC_36: p11, 123–24 The first clause of the long sentence is out of place, it is an outlook and would fit better at the end of the conclusions.

AC_36: Sentence has been move to the conclusions section.

RC_37: p12, 12 To which method do the R^2 and the RMSE value belong?

AC_37: Both methods yielded similar results. R^2 was the same and RMSE for Brutsaert (1975) and Jin et al. (2006) was 26 Wm^{-2} and 27 Wm^{-2} , respectively. This has been clarified in the text.

RC_38: p12, 11–7 You found that the new method was not better than the original Brutsaert (1975) formula. However, this does not necessarily imply that the Brutsaert (1975) method is good. I would like to see a discussion of limitations and other potential approaches.

AC_38: Differences between methods for estimating clear sky incoming longwave radiation continue to be evaluated over different climate zones (e.g., Choi et al., 2008) and indicate that discrepancies tend to be relatively small compared to uncertainty in modelling the turbulent fluxes. Therefore, a detailed discussion is not warranted for this analysis (see also response above).

RC_39: p12, l18 What is the 'evaluation subset'?

AC_39: This has been clarified in section 4.2 "Model inputs and evaluation datasets".

RC_40: p12, l30–32 The BR and RES methods need to be explained in the methods section. How does this description relate to the Priestley–Taylor approach you explain in the methods? Do the two methods refer to the canopy or the soil LE (eq. 10, 11)?

AC_40: BR (Bowen Ratio) and RES (Residual) methods have been referenced in the previous paragraph and they are intended to address the lack of closure of the flux station data used to evaluate the TSEB method. We compare TSEB to closed fluxes since the model requires energy balance closure while the measurements of H and LE using eddy covariance technique underestimate these fluxes by 10-20% based on comparison with available energy (Rn-G).

We used two methods:

1-a distribution of residual according to Bowen Ratio, with the acronym BR (Twine et al. 2000 and Foken 2008);

2- and LE was recalculated as the residual, with the acronym RES (Li et al., 2008).

In order to clarify the text for these methods, we have introduced these acronyms in the previous sentence. These methods are well explained in these papers and, for the sake of brevity, we prefer to refer the reader to the original references.

RC_41: p13, l26 Is the fraction of vegetation cover not estimated from the PAR budget? Please explain this in the methods! How sensitive is the model to LAI?

AC_41: The fraction of vegetation cover (Eq. 3) is computed using LAI and not PAR. We have clarified this in the text.

RC_42: p13, l30 Is f_G a sensitive parameter?

AC_42: The value of f_G modifies the estimated canopy transpiration (LEC) via the Priestley-Taylor parameterization (Eq. 10). It reduces LEC in direct proportion to its magnitude and has been used to adjust LEC based on crop phenology in other studies (e.g., Guzinski et al., 2015).

RC_43: p14, l26 As the interannual variability is not mentioned in the results, it should not be mentioned here.

AC_43: We have replaced "interannual" by "seasonal"

RC_44: p15, l3 'other models' is unclear. Do you mean 'G computation from RN'?

AC_44: Yes, this has been clarified in the text.

RC_45: p15, l3 As some readers start with reading the conclusions, it would be good to repeat that **_PTC** is used to estimate ET.

AC_45: This has been added in the text.

RC_46: p15, l6 Was the model sensitive to LAI? I would be surprised, as LAI (in the model) does not influence ET, albedo, or any of the other major fluxes. Otherwise this conclusion is not valid.

AC_46: LAI is used by TSEB (Eq. 3) to partition TRAD into soil and canopy temperature components, thus, it influences surface energy flux partitioning between the canopy and soil/substrate. The value of LAI also influences the radiation divergence and wind profile through the canopy layer and ultimately the soil and canopy aerodynamic resistances (Kustas and Norman, 1999;2000).

RC_47: p15, l8–10 On which result do you base this conclusion?

AC_47: We base this conclusion on the fact that the remote sensing-based TSEB model is able to capture the vegetation seasonal dynamics and contains the main factors (LST, LAI, vegetation height/roughness) affecting H and LE partitioning. Thus with a multi-year time series of remote sensing observations from satellites are able to detect changes in vegetation cover conditions (LAI, canopy height and roughness) which in turn can affect LST and hence energy flux partitioning. This permits monitoring the impact of vegetation cover changes on the water and energy cycle at synoptic scales with satellite data.

RC_48: p15, l11–14 This seems very abstract. Maybe you could rather conclude on how to integrate more satellite data to apply the model to the regional scale.

AC_48: Methods described in this sentence are designed to estimate surface energy fluxes with satellite data. We have clarified this in the text.

RC_49: Figure 3 This graph is very important. However, it would be great if you could add uncertainties, or at least standard deviations.

AC_49: Standard deviations for the mean values have been added to this figure.

RC_50: Figures 4–6 In the caption, PTC should be a subscript. This way of plotting does not allow an evaluation of G, one of your main focusses. Also, it is impossible to tell the accuracy of LE. I suggest to use just one variable per panel and indicate the point density with colour (heat map). As this will result in four times more panels, I suggest to remove Figure 5 as the additional information is small.

AC_50: PTC has been subscripted.

AC_50: Difference statistics between modelled and measured energy balance components are provided in tables 3 through 6. Having separate graphs comparing LE, H, RN and G would make it more difficult for the reader to have a sense of the relative magnitudes and scatter between the measured and modelled energy balance components. Showing the results in this manner gives the reader a better sense of the relative modelled-measured differences and which fluxes is the scatter the largest and most significant in the four components.

RC_51: Figure 7 The figure caption should be self explanatory. Please define fG.

AC_51: This has been added in the caption.

RC_52: Figure 8 I would prefer to see a sample time series to 5-day averages of multiple stations.

AC_52: 5-day averaged fluxes displayed in the figures more readily indicates the seasonal behaviour of TSEB over the whole study period. A sample time series is too noisy and does not allow the seasonal dynamics of surface energy fluxes and energy partitioning to be easily determined or illustrated.

RC_53: Figure 9 Change the symbols to make the figure easier to read. With the tiny legend and the turned figure it is impossible. I would suggest to have the same symbol for the same variable, once filled (for observed) and once empty (for modelled).

AC_53: The figure has been turned, the legend has been increased in size and the symbols have been refilled.

RC_54: Table 1 Space missing between Longwave and incoming; the captions says 'Average and standard deviation for the input values were computed for each period and for each site.' However, there is just one value per site given. Which period is it for?

AC_54: This has been corrected in the text.

AC_54: Average and standard deviations reported in this table were computed using all selected data from the full period of model evaluation (Period row) for each flux station. This has been clarified in the caption.

RC_55: Table 3 MAPD not MADP

AC_55: This has been corrected in the text.

RC_56: Table 5–6 One H misses the subscript.

AC_56: Sensible heat (H) is not missing the subscript. When using the residual method observed (from the flux tower) H is evaluated against modelled H.

Reviewer #2 comments

RC_1: The authors articulate a good case for undertaking their research and there is adequate acknowledgement of the previous literature although a summary of previous Arctic modelling that is relevant to your choice of model would be advantageous. They then propose an aim to evaluate the performance of the model during the Arctic growing season. However, it is unclear to me as to why you are doing this and what the ultimate goal is? Could you articulate what the big picture implications are in the introduction? In addition, I think you need to add an argument as to why this particular model as there are so many potential models with different scales and different functions. Why not use a process-based land surface model where you can relate the differences in model versus obs with processes rather than in your case changing a few parameters to get a better fit?

AC_1: We agree with the reviewer that the big picture motivation for evaluating TSEB performance over the Arctic tundra was not well described in the original submission, nor was our vision for upscaling to regional coverage. Our motivation is now better described in the final paragraphs of the introduction. In short, the TSEB forms the land surface model in a regional remote sensing energy balance system (ALEXI), used to model energy fluxes and ET from continental to global scales. ALEXI is currently used in NOAA OSPO's GET-D modeling system for North America (<http://www.ospo.noaa.gov/Products/land/getd/index.html>), and a prototype global modeling system is under development. ALEXI output has been evaluated over CONUS and lower latitude sites in Europe, but has not to date been tested over tundra ecosystems – constituting a significant fraction of the global land cover. Our primary goal in this paper is to evaluate TSEB performance over tundra, and to identify refinements that could be incorporated into the regional/global ALEXI system.

This motivation is now more clearly outlined in the introduction. We also provide a rationale for investigating a diagnostic flux system, which can be compared in future studies to process-based prognostic model output. Hain et al. (2015) performed a comparison of ALEXI and Noah latent heat flux estimates over CONUS and found the TSEB was able to diagnose missing moisture source/sink processes in the prognostic model (e.g., due to irrigation, shallow groundwater, etc). This motivation for focus on a diagnostic approach is also now provided within the introduction.

AC_1: TSEB has been already compared with other methodologies showing superior performance (e.g., Timmermans et al., 2007; Choi et al., 2009; Tang et al., 2011). This has also been included in the text.

RC_2: The authors use measured shortwave radiation yet estimate long wave radiation from observed air and land surface temperatures. I would have thought that this is problematic for Arctic environments and could result in a large error in the net radiation. Given that highly accurate net radiation and soil heat flux measurements are needed for this approach, what is error associated with estimating long wave radiation in the model?

AC_2: Upwelling longwave radiation was computed using T_{RAD} from the four component net radiation sensor and the Apogee IR sensors in each tower. Downwelling longwave radiation computed through Eq. 13 and estimation errors were reported in section 6.2, and showed a RMSE of $26 \text{ W}\cdot\text{m}^{-2}$.

RC_3: In addition, the authors assume that G is a constant fraction of net radiation. This assumption is untested and there is clearly a large uncertainty in the probable fraction into G due to differences in surface properties such as soil type and moisture conditions as the authors point out, but particularly also the composition and structure of the various organic layers which are ubiquitous across the Arctic. It is well understood that the properties of moss and organic materials in particular influence the thermal and hydrological properties of the soil greatly. Therefore, I would like to see a more formalised assessment of the relative uncertainty in the calculation of G and R_n .

AC_3: In the original TSEB formulation, a simple approach based on the relationship between G and R_{NS} was used (Eq. 13). For continental-to-global applications of the TSEB, we are indeed finding that variations in the main parameters of the G formulation are required – for example over rock or desert sands. However, as is explained in section 3.2 “Refinements in soil heat flux parameterization”, here we developed a new simple approach to estimate G based on a phase shift between LST and G to avoid errors using a constant fraction of net radiation over the diurnal cycle. The modifications derived here help to better capture thermal characteristics of the tundra substrate. Moreover, this method also investigates use of new scaling parameters that better reflect the thermal properties of the tundra soils, as noted by the reviewer.

RC_4: The authors give a mean value of 0.14 for cG and 0.92 for α_{PTC} over the Arctic tundra. There is a rather a lot of handwaving here to suggest a single value for the entire Arctic tundra. What was the range of values across different vegetation types in the Arctic tundra. What was the error around the mean for this value? In addition what is the influence of changing cover over the growing season on both these values?

AC_4: A standard deviation has been included in the text for α and G values.

AC_4: The initial values of the PTC use in this paper were the original value of 1.26 used in other TSEB applications and a value of 0.92 averaged from the main references found in the literature focused on Arctic tundra. As a starting point for the model we consider them applicable for areas of the Arctic with similar vegetation conditions. To clarify this within the text, the following paragraph has been added in section 2: “Under stress conditions, TSEB iteratively reduces α_{PTC} from its initial value. The TSEB model requires both a solution to the radiative temperature partitioning (Eq. 2) and the energy balance (Eqs. 6 and 7), with physically plausible model solutions for soil and vegetation temperatures and fluxes. Non-physical solutions, such as daytime condensation at the soil surface (i.e., $LE_S < 0$), can be obtained under conditions of moisture deficiency. This happens because LE_C is overestimated in these cases by the Priestley–Taylor parameterization, which describes potential transpiration. The higher LE_C leads to a cooler T_C and T_S must be accordingly larger to satisfy Eq. (7). This drives H_S high, and the residual LE_S from Eq. (11) goes negative. If this condition is encountered by the TSEB scheme, α_{PTC} is iteratively reduced until $LE_S \sim 0$ (expected for a dry soil surface). However there are instances where the vegetation is not transpiring at the potential rate but is not stressed

due to its adaption to water and climate conditions (Agam et al., 2010) or the fact that not all the vegetation is green or actively transpiring (Guzinski et al., 2013).”

RC_5: The use of MODIS LAI is particularly problematic in Arctic areas and it has been noted that the largest discrepancies in MODIS LAI are at Arctic tundra sites where the MODIS product overestimates woody cover proportions. Given that you have no LAI observations you cannot make any conclusions about how they relate to fPAR for example on page 13 line 30. What specific product was used, was it the 250 m resolution? What was the spatial extent of your footprint for this dataset and how does that relates to the spatial separation of your sites? Specifically which QC flags were used? How were gaps treated in the timeseries? Perhaps use MODIS fPAR. Given you have tower measurements of this you could validate the MODIS fPAR and assess the error here.

AC_5: The specific MODIS products used, and treatment of gap-filling and QC flags, are now more completely described in section 4.2.2.

RC_6: It is not clear as to how you distinguish between canopy and soil in these Arctic systems for the TSEB model. What do you define as soil and what is canopy? You have no significant woody vegetation to form a canopy in the first place. The surface layer consists of mosses, lichen, Forbes and shrubs and forms a continuous layer that cannot be partitioned into soil and canopy. I suspect in general you don't have any bare soil at your sites. Hence I'm not sure why you are using a two layer model here in the first place? Can you justify the use of a two layer model here? Therefore the assumption that fPAR is equivalent to fG is not robust. To use this you will need to demonstrate clearly that this is the case. Do you even need a two layer model? Perhaps evaluate the usefulness of this type of model in this type of environment.

AC_6: The tundra canopy in the region where we have the tower measurements is dominated by a shrub canopy having an average height of 0.4 m. This overstory is likely to strongly affect the energy exchange and divergence of radiation and wind reaching the moss/lichen surface while the moss/lichen understory will act similar to a “bare soil” surface being aerodynamically smooth. The energy balance of the moss/lichen surface is computed using a “bare soil” aerodynamic resistance for the sensible heat flux based on the “moss/lichen” temperature derived from Eq. (2), and with net radiation reaching this surface along with the estimated G term, the residual LE would then represent the mosses/lichen water use instead of bare soil. An assumption is that the soil resistance formulation is applicable to the moss/lichen understory. Given that the temperature partitioning derived from Eq. (2) which will yield a moss/lichen substrate temperature, significantly impacts the flux partitioning, using TSEB is assumed to be a reasonable approach for this ecosystem.

AC_6: As it was explained at the beginning of the reviews, f_G has been estimated using Guzinsky et al. (2013) methodology. This has been clarified in section 2.

RC_7: The description of the eddy covariance data is minimal. What software was used to process the data and what algorithms and parameters were used? Exactly what quality flags were filtered?

AC_7: The treatment of the EC data has now been expanded on in Section 4.2.3.

RC_8: What percentage of data were excluded due to different quality control previously mentioned as well as the three criteria mentioned.

AC_8: The first quality control excluded 20% of the data, accounting for inaccuracies in both meteorological and eddy covariance data. The second filter excluded 52% of the data due to summer rainy conditions in the Arctic. After the precipitation filter, 10% of data was excluded because of a balance closure for 30 min timesteps less than 70%. Finally, to account for daily conditions ($R_n > 100 \text{ W} \cdot \text{m}^{-2}$ filter), around 50% of the remaining data was excluded.

RC_9: How were gaps in the data filled and worthy gap filled data used in the analysis?

AC_9: No gap filled data was used in this study; this was clarified in the text. Although gap filled data would have increase the final amount of data to evaluate the model, we preferred to have less data that are more reliable since they were derived from the measurements.

RC_10: The criteria of a surface energy balance closure of greater than 70% doesn't instill a lot of confidence in the measurements. I would assume from this that the energy balance closure is quite low. This is probably due to the difficulty in measuring the soil heat flux.

AC_10: As mentioned in section 6.3, "the average energy balance closure using half-hour periods for the evaluation dataset was 88% which is in agreement with the average closure of 90% for these flux stations, (Euskirchen et al., 2012)".

RC_11: The measures of performance are relatively standard so I don't think you need to include the formulas here but just cite a previous reference.

AC_11: We prefer to keep the formulas; we found that sometimes it is useful for the reader to have them in the text to better interpret the results.

RC_12: The distribution of residual energy based on the Bowen ratio is not a common practice and the community in general prefers to see the original data being used. This is overwhelmingly important in this environment where there are very large errors in measurements of G and also R_n , both of which go into the available energy term. Errors in these will propagate into errors in the turbulent heat flux terms if you force them based on the bon ratio. Calculating LE as the residual of the surface energy balance equation is even more problematic as it is the sole term carrying all errors in the other terms. I would insist on redoing the analysis using only the original data and not presenting the other methods because they are so error prone.

AC_12: As explained in the text (section 6.3), lack of closure may be explained by instrument and methodological uncertainties, insufficient estimation of storage terms, unmeasured advective fluxes, landscape scale heterogeneity or instrument spatial representativeness, among others (Lund et al., 2014;Stoy et al., 2013;Foken et al., 2011;Foken, 2008;Wilson et al., 2002).

Currently, there is no uniform answer on how to deal with non-closure of the energy balance in eddy covariance datasets, and methods for analyzing the reasons for the lack of closure are still under discussion (Foken et al., 2011). More recently there is evidence that non-orthogonal sonics underestimate vertical velocity causing under-measurement of H and LE on the order of 10% (Kochendorfer et al., 2012; Frank et al., 2013), although this is still being debated (Kochendorfer et al., 2013).

This is the reason why in the current study a distribution of residual according to the Bowen ratio (BR) method was applied as suggested by Twine et al. (2000) and Foken (2008). In addition, LE was recalculated as the residual (RES) of the surface energy budget used in previous TSEB evaluations (Li et al., 2008).

Foken et al. (2011) concluded that the different footprints of radiation, soil heat flux, and turbulent flux measurements, including the storage terms, which were postulated earlier to be a reason, have no significant influence on the energy balance closure results. In addition, the sonic anemometer and gas analyzer used in this study are Type A instrument have a typical accuracy between 5% and 10% for sensible and latent heat flux estimation, respectively while shortwave radiation and longwave radiation measure with the four components net radiometer have a 1% and 20 $\text{W}\cdot\text{m}^{-2}$ accuracy (Foken, 2008). Additionally, the ground heat flux, including the storage term in the upper soil layer, can be determined with acceptable accuracy under most conditions (Foken, 2008). In our case we have a complete set of instrumentation to estimate G including soil bulk density data at each flux tower site.

RC_13: Table 2 shows the TCAV at 2 cm but this is usually an integrated measure with probes at two and 4 cm. Please check this.

AC_13: This has been clarified in the text. TCAV were placed in the soil at 2 and 4 cm depths.

RC_14: G is hard to measure. There is a great uncertainty in measurements of G in the tundra because traditional heat flux plates are made with an assumed thermal conductivity for loamy soils but we know in the tundra that this is primarily organic heat and moss which has a significantly lower thermal conductivity. Therefore self-calibrating heat flux plates or corrections are required. Can you quantify the uncertainty in your ground heat flux measurements which is an important term because it feeds directly into the energy balance?

AC_14: We have used self-calibrating soil heat flux plates. This has been clarified in Table 2. In addition, we have used the calorimetric method using soil bulk density data for each site to account for soil heat storage as it was explained in section 4.2 “Model inputs and evaluation datasets”. This method has been also applied for Lund et al. (2014) for tundra conditions.

RC_15: How did you account for these in the correction of the soil heat flux plates? At what depth did you have the heat flux plates placed? I see they were 8 cm but is that below the surface in the moss? If so then your heat flux plates are not in soil but in organic material. You should use the appropriate bulk density not the soil bulk density. Also it appears that you only have one heat flux plate measurement per site which is insufficient given the spatial heterogeneity in the surface. As previously mentioned the thermal conductivity of the heat flux plate is manufactured to a standard soil which will not be

representative of what you are measuring in. This will all result in very large errors in the observed soil heat flux.

AC_15: As explained above, we have used self-calibrating soil heat flux plates, TCAV water reflectometers to estimate G. All instruments are placed in the soil and not in the moss layer. We have used the calorimetric method using soil bulk density data for each site to account for soil heat storage as it was explained in section 4.2 “Model inputs and evaluation datasets”. This method has been also applied for Lund et al. (2014) for tundra conditions. The soil bulk density was already mentioned in the paper and it is $758 \text{ kg}\cdot\text{m}^{-3}$, $989 \text{ kg}\cdot\text{m}^{-3}$ and $1038 \text{ kg}\cdot\text{m}^{-3}$ for Fen, Tussock and Heath flux stations, respectively.

AC_15: We agree with the reviewer that having more soil heat flux plates, TCAV and water reflectometers will improve the soil heat flux calculation. In table 2 we only listed the instruments but not the number of instruments per site. We have four self-calibrating soil heat flux plates, two water reflectometers and two thermocouple averaging soil temperature probes per flux station. This has been clarified in table 2. Similar instrumentation (same amount of instrumentation) is also used in many FLUXNET sites to address the spatial heterogeneity in the surface the soil.

RC_16: Please provide a thorough estimate of error and uncertainty for this particular important measurement. In addition, what is the uncertainty (random and model) in the fluxes for each of the sites?

AC_16: Soil heat flux model error is reported in detail under Section 6.1

RC_17: Given the difficulty in measuring G and the errors associated with that it may be worth trying to take G as a residual of the surface energy balance.

AC_17: In our case, G is a relatively small term compared with other fluxes, and as we explained before, lack of closure is likely to occur due to methodological uncertainties, insufficient estimation of storage terms, etc. when processing eddy covariance data (sensible and latent heat fluxes).

RC_18: As mentioned in the summary there is a lot of focus on model error and performance. However, these comparisons are with often in different types of models in different ecosystems which is like comparing apples and oranges. Most published models will have some reasonable performance but we should move away from a simple reporting of the error to include better and more robust benchmarking of models. For example, this model could be compared against a simple empirical model to assess quantitatively whether the model performs any better than a simple model with local meteorological drivers. Recent papers have started to do and I suggest this is something that you could do to strengthen your paper. For example see:

Whitley, R., Beringer, J., Hutley, L., Abramowitz, G., De Kauwe, M. G., Duursma, R., Evans, B., Haverd, V., Li, L., Ryu, Y., Smith, B., Wang, Y.-P., Williams, M. and Yu, Q.: A model inter-comparison study to examine limiting factors in modelling Australian

tropical savannas, *Biogeosciences Discuss.*, 12(23), 18999–19041, doi:10.5194/bg-12-18999-2015, 2015.

Luo, Y. Q., Randerson, J. T., Abramowitz, G., Bacour, C., Blyth, E., Carvalhais, N., Ciais, P., Dalmonech, D., Fisher, J. B., Fisher, R., Friedlingstein, P., Hibbard, K., Hoffman, F., Huntzinger, D., Jones, C. D., Koven, C., Lawrence, D., Li, D. J., Mahecha, M., Niu, S. L., Norby, R., Piao, S. L., Qi, X., Peylin, P., Prentice, I. C., Riley, W., Reichstein, M., Schwalm, C., Wang, Y. P., Xia, J. Y., Zaehle, S. and Zhou, X. H.: A framework for benchmarking land models, *Biogeosciences*, 9(10), 3857–3874, doi:10.5194/bg-9-3857-2012, 2012.

AC_18: Ultimately, this would be a goal for a follow-on paper. This paper focused on the utility of adapting/refining the TSEB land surface scheme for the Arctic tundra region represented by the flux tower sites used in this study. This is the reason we used Kalma et al. (2008) study as a robust benchmark for evaluating the performance of the TSEB relative to a large number of surface energy balance models using land surface temperature. In this paper, methods for estimating evaporation from landscapes, regions and larger geographic extents, with remotely sensed surface temperatures were reviewed, and uncertainties and limitations associated with those estimation methods were highlighted. In addition, particular attention was given to the validation of such approaches against ground based flux measurements. An assessment of some 30 published validations summarized in Kalma et al (2008) ranging from complex physical and analytical methods to empirical and statistical approaches) indicates a robust model should yield an average root mean square error (RMSE) value of around 50 W m^{-2} or less in estimated hourly turbulent fluxes H and LE during daytime conditions. The results from the current study yield RMSE values that fall generally below 50 W m^{-2} and hence considered a robust thermal-based energy balance model for the Arctic tundra.

RC_19: Page 14, line 3, the effect of what over the model? Mosses? In addition in this paragraph although you should not use the modus LA it is still consistent with seasonal growth of deciduous shrubs in particular. It is not inconsistent to have a constant fPAR where almost all incoming PAR is absorbed. The Arctic environment is highly adapted to absorbing as much energy as it can. As the leaf area of the shrubs increases during the summer the absorbed PAR is spread out amongst a greater leaf area but the fraction of fPAR remains the same.

AC_19: The lack of FAPAR consistency has been addressed in previous comments by using Guzinski et al. (2013) approach.

RC_20: Given this is a two layer model where are the results from the canopy and soil components.

AC_20: Although the TSEB model components the overstory and understory component fluxes, there are no measurements available to evaluate the reliability of the partitioning. This is a project planned for a future study when measurements of the component fluxes are available.

References

Asner, G. P.: Biophysical and Biochemical Sources of Variability in Canopy Reflectance, *Remote Sens Environ*, 64, 234–253, 1998.

Choi, M. H., Jacobs, J. M., and Kustas, W. P.: Assessment of clear and cloudy sky parameterizations for daily downwelling longwave radiation over different land surfaces in Florida, USA, *Geophys Res Lett*, 35, Artn L20402 10.1029/2008gl035731, 2008.

Choi, M., Kustas, W.P., Anderson, M.C., Allen, R.G., Li, F., and Kjaersgaard, J.P., An intercomparison of three remote sensing-based surface energy balance algorithms over a corn and soybean production region (Iowa, U.S.) during SMACEX. *Agric. Forest Meteorol.* 149: 2082–2097. 2009.

Euskirchen, E. S., Bret-Harte, M. S., Scott, G. J., Edgar, C., and Shaver, G. R.: Seasonal patterns of carbon dioxide and water fluxes in three representative tundra ecosystems in northern Alaska, *Ecosphere*, 3, art4, 10.1890/es11-00202.1, 2012.

Foken, T.: The energy balance closure problem: an overview, *Ecol Appl*, 18, 1351-1367, doi:10.1890/06-0922.1, 2008.

Foken, T., Aubinet, M., Finnigan, J. J., Leclerc, M. Y., Mauder, M., and U, K. T. P.: Results of a Panel Discussion About the Energy Balance Closure Correction for Trace Gases, *B Am Meteorol Soc*, 92, Es13-Es18, doi:10.1175/2011BAMS3130.1, 2011.

Fisher, J. B., Tu, K. P., and Baldocchi, D. D.: Global estimates of the land-atmosphere water flux based on monthly AVHRR and ISLSCP-II data, validated at 16 FLUXNET sites, *Remote Sens Environ*, 112, 901-919, 10.1016/j.rse.2007.06.025, 2008.

Frank, J. M., Massman, W. J., and Ewers, B. E.: Underestimates of sensible heat flux due to vertical velocity measurement errors in non-orthogonal sonic anemometers, *Agr Forest Meteorol*, 171, 72-81, doi:10.1016/j.agrformet.2012.11.005, 2013.

Guzinski, R., Anderson, M. C., Kustas, W. P., Nieto, H., and Sandholt, I.: Using a thermal-based two source energy balance model with time-differencing to estimate surface energy fluxes with day–night MODIS observations, *Hydrol Earth Syst Sc*, 17, 2809-2825, doi:10.5194/hess-17-2809-2013, 2013.

Guzinski, R., Nieto, H., Stisen, S., and Fensholt, R.: Inter-comparison of energy balance and hydrological models for land surface energy flux estimation over a whole river catchment, *Hydrol Earth Syst Sc*, 19, 2017-2036, 10.5194/hess-19-2017-2015, 2015.

Huemmrich, K. F., Gamon, J. A., Tweedie, C. E., Oberbauer, S. F., Kinoshita, G., Houston, S.,

Kuchy, A., Hollister, R. D., Kwon, H., Mano, M., Harazono, Y., Webber, P. J., and Oechel, W. C.: Remote sensing of tundra gross ecosystem productivity and light use efficiency under varying temperature and moisture conditions, *Remote Sens Environ*, 114, 481-489, 10.1016/j.rse.2009.10.003, 2010.

Kalma, J. D., McVicar, T. R., and McCabe, M. F.: Estimating Land Surface Evaporation: A Review of Methods Using Remotely Sensed Surface Temperature Data, *Surv Geophys*, 29, 421-469, doi:10.1007/s10712-008-9037-z, 2008.

Kochendorfer, J., Meyers, T. P., Frank, J., Massman, W. J., and Heuer, M. W.: How Well Can We Measure the Vertical Wind Speed? Implications for Fluxes of Energy and Mass, *Bound-Lay Meteorol*, 145, 383-398, doi:10.1007/s10546-012-9738-1, 2012.

Kochendorfer, J., Meyers, T. P., Frank, J. M., Massman, W. J., and Heuer, M. W.: Reply to the Comment by Mauder on “How Well Can We Measure the Vertical Wind Speed? Implications for Fluxes of Energy and Mass”, *Bound-Lay Meteorol*, 147, 337-345, doi:10.1007/s10546-012-9792-8, 2012.

Kustas, W. P. and Norman, J. M. Evaluation of soil and vegetation heat flux predictions using a simple two-source model with radiometric temperatures for partial canopy cover. *Agricultural and Forest Meteorology*. 94:13-29. 1999.

Kustas, W. P. and Norman, J. M. A two-source energy balance approach using directional radiometric temperature observations for sparse canopy covered surfaces. *Agronomy Journal*. 92:847-854. 2000.

Li, F. Q., Kustas, W. P., Prueger, J. H., Neale, C. M. U., and Jackson, T. J.: Utility of remote sensing-based two-source energy balance model under low- and high-vegetation cover conditions, *J Hydrometeorol*, 6, 878-891, doi:10.1175/Jhm464.1, 2005.

Lund, M., Hansen, B. U., Pedersen, S. H., Stiegler, C., and Tamstorf, M. P.: Characteristics of summer-time energy exchange in a high Arctic tundra heath 2000-2010, *Tellus B*, 66, doi:10.3402/Tellusb.V66.21631, 2014.

Norman, J. M., Kustas, W. P., Prueger, J. H., and Diak, G. R.: Surface flux estimation using radiometric temperature: A dual-temperature-difference method to minimize measurement errors, *Water Resour Res*, 36, 2263, doi:10.1029/2000wr900033, 2000.

Stoy, P. C., Williams, M., Spadavecchia, L., Bell, R. A., Prieto-Blanco, A., Evans, J. G., and van Wijk, M. T.: Using Information Theory to Determine Optimum Pixel Size and Shape for Ecological Studies: Aggregating Land Surface Characteristics in Arctic Ecosystems, *Ecosystems*, 12, 574-589, 10.1007/s10021-009-9243-7, 2009.

Tang., R., Li, Z-L., Jia, Y., Li, C., Sun, X., Kustas, W.P. and Anderson, M.C. An intercomparison of three remote sensing-based energy balance models using Large Aperature

Scintillometer measurements over a wheat-corn production region. *Remote Sensing of Environment*, 115:3187-3202, 2011.

Timmermans, W. J., Kustas, W. P., Anderson, M. C., and French, A. N.: An intercomparison of the Surface Energy Balance Algorithm for Land (SEBAL) and the Two-Source Energy Balance (TSEB) modeling schemes, *Remote Sens Environ*, 108, 369-384, 10.1016/j.rse.2006.11.028, 2007.

Twine, T. E., Kustas, W. P., Norman, J. M., Cook, D. R., Houser, P. R., Meyers, T. P., Prueger, J. H., Starks, P. J., and Wesely, M. L.: Correcting eddy-covariance flux underestimates over a grassland, *Agr Forest Meteorol*, 103, 279-300, doi:10.1016/S0168-1923(00)00123-4, 2000.

Wilson, K., Goldstein, A., Falge, E., Aubinet, M., Baldocchi, D., Berbigier, P., Bernhofer, C., Ceulemans, R., Dolman, H., Field, C., Grelle, A., Ibrom, A., Law, B. E., Kowalski, A., Meyers, T., Moncrieff, J., Monson, R., Oechel, W., Tenhunen, J., Williams, M., Rastetter, E. B., Shaver, G. R., Hobbie, J. E., Carpino, E., and Kwiatkowski, B. L.: Primary production of an arctic watershed: An uncertainty analysis, *Ecol Appl*, 11, doi:1800-1816, 10.1890/1051-0761, 2001.

Zhan, X., Kustas, W. P., and Humes, K. S.: An intercomparison study on models of sensible heat flux over partial canopy surfaces with remotely sensed surface temperature, *Remote Sens Environ*, 58, 242-256, Doi 10.1016/S0034-4257(96)00049-1, 1996.

Estimation of surface energy fluxes in the Arctic tundra using the remote sensing thermal-based Two-Source Energy Balance model

Jordi Cristóbal^{1,2}, Anupma Prakash¹, Martha C. Anderson³, William P. Kustas³, Eugénie S. Euskirchen⁴, Douglas L. Kane²

5 | ¹Geophysical Institute. University of Alaska Fairbanks, Fairbanks, Alaska, 99775, USA

²Institute of Northern Engineering. Water Environmental Research Center, University of Alaska Fairbanks, Fairbanks, Alaska, 99775, USA

³Hydrology and Remote Sensing Laboratory, United States Department of Agriculture, Agriculture Research Service, Beltsville, Maryland, 20705, USA

10 | ⁴Institute of Arctic Biology. University of Alaska Fairbanks, Fairbanks, Alaska, 99775, USA

Correspondence to: Jordi Cristóbal (j.cristobal@alaska.edu)

Abstract. The Arctic has become generally a warmer place over the past decades leading to earlier snow melt, permafrost degradation and changing plant communities. Increases in precipitation and local evaporation in the Arctic, known as ~~one of~~ the acceleration components of the hydrologic cycle, coupled with land cover changes, have resulted in significant changes in the regional surface energy budget. Quantifying spatiotemporal trends in surface energy flux partitioning is a key to forecasting ecological responses to changing climate conditions in the Arctic ~~regions~~. An extensive local evaluation of the two-source energy balance model (TSEB) - a remote sensing-based model using thermal infrared retrievals of land-surface temperature - was performed using tower measurements collected over different tundra types in Alaska in all sky conditions over the full growing season from 2008 to 2012. Based on comparisons with flux tower observations, refinements in the original TSEB net radiation, soil heat flux and canopy transpiration parameterizations were identified for ~~the unique~~-Arctic tundra ~~conditions~~. In particular, a revised method for estimating soil heat flux based on relationships with soil temperature was developed, resulting in significantly improved performance. These refinements result in mean turbulent flux errors ~~around~~generally less than 50 W·m⁻² at half-hourly timesteps, similar to errors typically reported in surface energy balance modelling studies conducted in more temperate climatic regimes. The MODIS LAI remote sensing product proved to be useful for estimating energy fluxes in Arctic tundra in the absence of field data. ~~This work builds on local biomass amount.~~ Model refinements found in this work at the local scale build toward a regional implementation of the TSEB model over Arctic tundra ecosystems, using thermal satellite remote sensing to assess response of surface fluxes to changing vegetation and climate conditions.

1 Introduction

30 | ~~Near surface or shelter level air~~Air temperatures in the Alaskan Arctic have shown a significant increase, especially in past decade (Serreze and Barry, 2011). Results from models forced with a range of climate scenarios from the Intergovernmental

Panel on Climate Change (IPCC) indicate that by the mid-21st century the permafrost area in the Northern Hemisphere is likely to decrease by 20–35% (Bates et al., 2008). In general, the Arctic has become a warmer place, leading to an acceleration of the hydrologic cycle, earlier snow melt, and drier soils due to permafrost degradation (~~ACIA, 2004; AMAP, 2012; Lammers et al., 2001; Vörösmarty et al., 2001~~(AMAP, 2012; Elmendorf et al., 2012; Rawlins et al., 2010; Sturm et al., 2001; Overduin and Kane, 2006; ~~Arendt et al., 2002~~)). Furthermore, the hydrologic response of the Arctic land surface to changing climate is dynamically coupled to the region’s surface energy balance (Vörösmarty et al., 2001), and ~~the~~ partitioning of energy fluxes plays an important role in modulating the hydrologic cycle of Arctic basins (Rawlins et al., 2010).

Evapotranspiration (ET, in units of mass, $\text{kg s}^{-1} \text{m}^{-2}$ or mm d^{-1}) or equivalently, latent heat flux (LE, in energy units, $\text{W}\cdot\text{m}^{-2}$), is an important component of both the land surface hydrologic cycle and surface energy balance. As an example, Kane et al. (2004) reported water loss due to ET in the Innvait Creek Basin in Alaska is about 74% of summer precipitation or 50% of annual precipitation, as estimated from water balance computations. Even though ET is a significant component of the hydrologic cycle in Arctic regions, it is poorly quantified in Arctic basins, and the bulk estimates do not accurately account for spatial and temporal variability due to vegetation type and topography (Kane and Yang, 2004). In the Arctic, values of ET or LE are usually either derived from field estimates (Kane et al., 1990; Mendez et al., 1998) or calculated purely from empirical or quasi-physical models such as those described by Zhang et al. (2000) and Shutov et al. (2006) using meteorological station forcing data. However, due to remoteness, harsh winter conditions and the high costs of maintaining ground-based measurement networks, the data currently collected are also ~~inconsistent~~ both temporally and spatially sparse.

~~Over at least the past three decades, Arctic ecosystems have shown evidence of “greening” (Xu et al., 2013; Jia et al., 2003), with about a 14% increase in peak vegetation for the Arctic tundra biome (Bhatt et al., 2010).~~ In Arctic tundra ecosystems, several factors have contributed to the vegetation change such as increased extent of severe fires, increased extent in deciduous vegetation or shrub encroachment in tundra ecosystems (Myers-Smith et al., 2011; Sturm et al., 2001), among others. Over at least the past three decades, Arctic ecosystems have shown evidence of “greening” (Myers-Smith et al., 2011; Sturm et al., 2001)(Xu et al., 2013; Bhatt et al., 2010), among others, with about a 17% increase in peak vegetation greenness for the Arctic tundra biome (Jia et al., 2003). Moreover, the forest-tundra transition zone is ~~continually~~ observed to be moving further north, tree heights are increasing, and shrubs are becoming denser and taller (ACIA, 2004; AMAP, 2012). These changes in vegetation will have an important impact on the surface energy balance, especially in areas where shrubs have made their appearance in former tundra vegetation. This increase in leaf area index, together with canopy height, and changes in the distribution of canopy elements, will augment the multiple scattering and absorption of radiation, likely resulting in a lower albedo (Beringer et al., 2005). ~~Also, although more detailed observations and measurements, particularly for the beginning of the snow-free period and peak growing season are needed (Williamson et al., 2016).~~ Also, according to Beringer et al. (2005), Bowen ratio increases from tundra to forested sites will result in an increasing dominance of sensible heat (H) as the primary energy source heating the atmosphere. In the case of a transition from tundra to tall shrub and then to

forest, H would likely increase during the growing season from ~15% to nearly 30%, respectively. This will have an important impact in the tundra energy partitioning, resulting in a positive feedback to the atmosphere that further warms the Arctic climate. However, the magnitude of changes in surface energy partitioning due to vegetation changes and resulting impact on local Arctic climate is still unclear and more research is needed to better understand these vegetation change-atmosphere dynamics (Eugster et al., 2000; Jung et al., 2010).

In the last two decades, surface energy balance methods have demonstrated their utility in modelling water availability using diagnostic retrievals of energy fluxes from *in situ* or remote sensing data, especially data acquired in the thermal infrared (TIR) region (Kalma et al., 2008). While remote sensing estimates of ET over the Arctic exist from global modelling systems (Mu et al., 2009; Zhang et al., 2010), these modelling systems typically do not compute the full energy balance. To estimate energy fluxes at local scales, on the order of hundreds of meters, initiatives such as FLUXNET (<http://fluxnet.ornl.gov/>) provide eddy covariance flux measurements at discrete sites situated in different ecosystems across the U.S. and globally. Unfortunately, there are few measurements sites in the Arctic (Mu et al., 2009), making the existing instrument network insufficient to capture pertinent details of the changing Arctic climate and landscape (ACIA, 2004; AMAP, 2012; Serreze and Barry, 2011; Vörösmarty et al., 2001). ~~Consequently, there is a strong need to focus on refining and evaluating models providing spatial distributed fluxes to facilitate more accurate spatio-temporal mapping of Arctic energy fluxes. Detailed process-based (prognostic) land-surface models can be also used to estimate coupled water and energy fluxes over landscapes (Duursma and Medlyn, 2012; Ek et al., 2003; Falge et al., 2005; Haverd et al., 2013; Smith et al., 2001; Vinukollu et al., 2012, among others); however, they may neglect important processes that are not known a priori. For example, Hain et al. (2015) demonstrated the value of comparing prognostic and TIR-based diagnostic latent heat flux estimates over the continental U.S. to diagnose moisture sources and sinks that were not well-represented in the prognostic modelling system.~~

~~The~~ Given the critical need to better understand the water and energy balance over tundra ecosystems, and the role of ~~changing climate and vegetation cover in driving these budgets, the~~ aim of this work is to evaluate ~~the performance of and refine~~ a diagnostic remote sensing energy balance approach, forced primarily by measurements of land surface temperature, for estimating surface energy fluxes during Arctic tundra growing season. The Two-Source Energy Balance (TSEB) model, proposed by Norman et al. (1995), serves as the land surface scheme in a regional Atmosphere-Land Exchange Inverse (ALEXI) modelling system, which uses TIR observations from geostationary and polar orbiting satellites to estimate surface fluxes from field to global scales (Anderson et al., 2011). ALEXI is currently implemented operationally over North America as part of NOAA's GOES Evapotranspiration and Drought Information System (GET-D; <http://www.ospo.noaa.gov/Products/land/getd/index.html>). ALEXI/TSEB has been demonstrated to work well over a range in vegetation and climate conditions; (Anderson et al., 2007, 2011; Choi et al., 2009; Sánchez et al., 2009; Tang, et al., 2011; Timmermans et al., 2007, among others) and superior performance to other remote sensing based surface energy balance methods (Choi et al., 2009; Tang, et al., 2011; Timmermans et al., 2007), but has not yet been examined for tundra

ecosystems ~~at characteristic of~~ high latitudes. ~~This TSEB land surface scheme has been coupled to a regional modelling system using geostationary and polar orbiting satellite data providing regional and continental scale fluxes and thus could potentially be applied to the Arctic for monitoring and mapping within~~ the surface energy balance (Anderson et al., 2011). ~~GET-D and global modelling domains.~~ In this study, the TSEB is ~~re~~evaluated locally, using in situ forcing data from three eddy covariance flux towers in all sky conditions (including clear sky, partially cloudy and overcast conditions) over Alaskan tundra sites during the growing season from 2008 to 2012. Vegetation amount is quantified using leaf area index, ~~NDVI and EVI~~ data from the Moderate Resolution Imaging Spectroradiometer (MODIS). The modelled energy balance is compared with measurements at three flux sites to ascertain modifications required to enhance ~~TSEB and ALEXI~~ performance over tundra ecosystems.

10 2 Two-Source Energy Balance model: an overview

Evapotranspiration (ET) can be estimated by surface energy balance models that partition the energy available at the land surface ($R_N - G$, where R_N is net radiation and G is the soil heat flux, both in $W \cdot m^{-2}$) into turbulent fluxes of sensible and latent heating (H and LE , respectively, in $W \cdot m^{-2}$):

$$LE + H = R_N - G, \quad (1)$$

15 where L is the latent heat of vaporization ($J \cdot kg^{-1}$) and E is ET ($kg \cdot s^{-1} \cdot m^{-2}$ or $mm \cdot s^{-1}$).

The model used in this study is the series version of the Two-Source Energy Balance (TSEB) scheme originally proposed by Norman et al. (1995), which has been revised to improve shortwave and longwave radiation exchange within the soil–canopy system and the soil–canopy energy exchange (Kustas and Norman, 1999, 2000). A list of the TSEB inputs can be found in Table 1. TSEB has been successfully applied over ~~rainfed~~rain fed and irrigated crops and grasslands in temperate and semi-arid climates (Anderson et al., 2012; Anderson et al., 2004; Cammalleri et al., 2012, 2010) but has not been previously applied over the Arctic tundra.

In the TSEB, directional surface radiometric temperature derived from satellite or a ground-based radiometer, $T_{RAD}(\theta)$ (K), is considered to be a composite of the soil and canopy temperatures, expressed as:

$$T_{RAD}(\theta) \approx [f_c(\theta)T_c^4 + (1 - f_c(\theta))T_s^4]^{1/4}, \quad (2)$$

25 where T_c is canopy temperature (K), T_s is soil temperature (K), and $f_c(\theta)$ is the fractional vegetation cover observed at the radiometer view angle θ . For a canopy with a spherical leaf angle distribution and leaf area index LAI, $f_c(\theta)$ can be estimated as:

$$f_c(\theta) = 1 - \exp\left(\frac{-0.5\Omega LAI}{\cos\theta}\right), \quad (3)$$

where the factor Ω indicates the degree to which vegetation is clumped as in ~~row~~row crops or sparsely vegetated ~~shrubland~~shrub land canopies (Kustas and Norman, 1999, 2000). The composite soil and canopy temperatures are used to compute the surface energy balance for the canopy and soil components of the combined land-surface system:

$$R_{NS} = H_S + LE_S + G, \quad (4)$$

$$5 \quad R_{NC} = H_C + LE_C, \quad (5)$$

where R_{NS} is net radiation at the soil surface, R_{NC} is net radiation divergence in the vegetated canopy layer, H_C and H_S are canopy and soil sensible heat flux, respectively, LE_C is the canopy transpiration rate, LE_S is soil evaporation, and G is the soil heat flux. The net shortwave radiation is calculated from the measured incoming solar radiation and the surface albedo, while net longwave radiation is estimated from the observed air and land surface temperatures, using the Stefan-Boltzmann

10 equation with atmospheric emissivity from the Brutsaert (1975) method.

By permitting the soil and vegetated canopy fluxes to interact with each other, Norman et al. (1995) derived expressions for H_S and H_C expressed as a function of temperature differences where:

$$H_S = \rho C_p \frac{T_S - T_{AC}}{R_{TS}}, \quad (6)$$

and

$$15 \quad H_C = \rho C_p \frac{\frac{T_C - T_{AC}}{R_{TC}} T_C - T_{AC}}{r_X}, \quad (7)$$

with the total sensible heat flux $H = H_C + H_S$ expressed as:

$$H = \rho C_p \frac{\frac{T_{AC} - T_A}{R_{TA}} T_{AC} - T_A}{r_A}, \quad (8)$$

20 where ρ is air density ($\text{kg}\cdot\text{m}^{-3}$), C_p is the specific heat of air ($\text{kJ}\cdot\text{kg}^{-1}\cdot\text{K}^{-1}$), T_{AC} is air temperature in the canopy air layer (K), T_A is the air temperature in the surface layer measured at some height above the canopy (K), R_{TX} is the total boundary layer resistance of the complete canopy of leaves ($\text{s}\cdot\text{m}^{-1}$), R_{SLS} is the resistance to sensible heat exchange from the soil surface ($\text{s}\cdot\text{m}^{-1}$) and R_{AIA} is aerodynamic resistance ($\text{s}\cdot\text{m}^{-1}$) defined by:

$$R_A = \frac{[\ln((z_U - d_O)/z_{OM}) - \Psi_M][\ln((z_T - d_O)/z_{OM}) - \Psi_H]}{k^2 u}, \quad (9)$$

25 In Eq. (9) d_O is the displacement height, u is the wind speed measured at height z_U , k is von Karman's constant (≈ 0.4), z_T is the height of the T_A measurement, Ψ_M and Ψ_H are the Monin-Obukhov stability functions for momentum and heat, respectively, and z_{OM} is the aerodynamic roughness length.

The original resistance formulations are described in more detail in Norman et al. (1995) with revisions described in Kustas and Norman (1999) and Kustas and Norman (2000). Weighting of the heat flux contributions from the canopy and soil components is performed indirectly by the partitioning of the R_N between soil and canopy and via the impact on resistance values from the fractional amount and type of canopy cover (see Kustas and Norman, 1999).

5 For the latent heat flux from the canopy, the Priestley–Taylor formula is used to initially estimate a potential rate for LE_C :

$$LE_C = \alpha_{PTC} f_G \frac{\Delta}{\Delta + \gamma} R_{NC}, \quad (10)$$

where α_{PTC} is a variable quantity related to the Priestley–Taylor coefficient (Priestley and Taylor, 1972), but in this case defined exclusively for the canopy component, which was suggested for row crops by Tanner and Jury (1976) and normally set to an initial value of 1.2, ~~f_G is the fraction of green vegetation,~~ Δ is the slope of the saturation vapour pressure versus temperature curve and γ is the psychrometric constant ($\sim 0.066 \text{ kPa } ^\circ\text{C}^{-1}$). ~~Under stress conditions, TSEB iteratively reduces α_{PTC} from its initial value (a thorough discussion of conditions f_G is the fraction of green vegetation that force a reduction in α_{PTC} ; according to Guzinski et al. (2013) and Fisher et al., (2008) can be found in Anderson et al. (2005) and Li et al. (2005)) estimated through the normalized difference vegetation index (NDVI) and the enhanced vegetation index (EVI);~~

$$15 \quad f_G = 1.2 \frac{EVI}{NDVI}, \quad 0 \leq f_G \leq 1, \quad (11)$$

~~Under stress conditions, TSEB iteratively reduces α_{PTC} from its initial value. The TSEB model requires both a solution to the radiative temperature partitioning (Eq. 2) and the energy balance (Eqs. 6 and 7), with physically plausible model solutions for soil and vegetation temperatures and fluxes. Non-physical solutions, such as daytime condensation at the soil surface (i.e., $LE_S < 0$), can be obtained under conditions of moisture deficiency. This happens because LE_C is overestimated in these cases by the Priestley–Taylor parameterization, which describes potential transpiration. The higher LE_C leads to a cooler T_C and T_S must be accordingly larger to satisfy Eq. (7). This drives H_S higher, and the residual LE_S from Eq. (12) can become negative. If this condition is encountered by the TSEB scheme, α_{PTC} is iteratively reduced until $LE_S \sim 0$ (expected for a dry soil/substrate surface). However there are instances where the vegetation is not transpiring at the potential rate but is not stressed due to its adaption to water and climate conditions (Agam et al., 2010) or the fact that not all the vegetation is green or actively transpiring (Guzinski et al., 2013) (a thorough discussion of conditions that force a reduction in α_{PTC} , can be also found in Anderson et al. (2005) and Li et al. (2005)).~~

The latent heat flux from the soil surface is solved as a residual in the energy balance equation:

$$LE_S = R_{NS} - G - H_S, \quad (12)$$

with G estimated as a fraction of the net radiation at the soil surface (c_G):

$$G = c_G R_{NS}, \quad (4213)$$

From midmorning to midday period, ~~when daytime TIR satellite imagery is typically acquired,~~ the value of c_G can be typically assumed to be constant (Kustas and Daughtry, 1990; Santanello and Friedl, 2003). In this case, a typical value of ~ 0.3 can be assumed for c_G based on experimental data from several sources (Daughtry et al., 1990). However, c_G value varies with soil type and moisture conditions as well as time, due to the phase shift between G and R_{NS} over a diurnal cycle (Santanello and Friedl, 2003).

3 TSEB formulation refinements for Arctic tundra

3.1 Downwelling longwave radiation estimation: effective atmospheric emissivity for all sky conditions

10 The original TSEB formulation estimates the downwelling longwave radiation component of R_N using the effective atmospheric emissivity (ε) method described in Brutsaert (1975) for clear sky conditions:

$$\varepsilon = C(e/T_A)^{1/7}, \quad (4314)$$

where e is the water pressure in millibars and T_A in K and C is 1.24 as in the original Brutsaert (1975) formulation. However, in this study TSEB is applied for all sky conditions, including clear sky, partially cloudy and overcast conditions. To estimate ε for all sky conditions Crawford and Duchon (1999) proposed a methodology that incorporated the Brutsaert (1975) clear-sky parameterization and the Deardorff (1978) cloudiness correction using a simple cloud modification introducing a cloud fraction term (clf) according to the following equation:

$$\varepsilon = \{clf + (1 - clf)[C(e/T_A)^{1/7}]\}, \quad (4415)$$

The clf is defined as:

$$20 \quad clf = 1 - s, \quad (4516)$$

where s is the ratio of the measured solar irradiance to the clear-sky irradiance. Shortwave clear-sky irradiance used in Eq. (4516) may be obtained through the methodology proposed by Pons and Ninyerola (2008), where incident clear-sky irradiance is calculated through a digital elevation model at a specific point during a particular day of the year taking into account the position of the Sun, the angles of incidence, the projected shadows, the atmospheric extinction and the distance from the Earth to the Sun.

25 For Arctic areas, Jin et al. (2006) suggested an improved formulation of C for clear sky conditions that can also be applied in Eq. (4415) for all sky conditions, defined as:

$$C = 0.0003(T_A - 273.16)^2 - 0.0079(T_A - 273.16) + 1.2983, \quad (4617)$$

In order to evaluate if the Jin et al. (2006) method offered more accurate estimates of ε for Arctic conditions, this method was compared to Brutsaert (1975) formulation used in TSEB, in both cases for all sky conditions using Eq. (415).

3.2 Soil Refinements in soil heat flux parameterization: c_G coefficient and definition of a new coefficient based on T_{RAD} : c_G coefficient

Currently there are several methodologies that allow estimating soil heat flux from tenths of centimetres to meters in depth in the Arctic tundra by using modelling or instrumentation at several depths (Lynch et al., 1999; Ekici et al., 2015; Jiang et al., 2015; Romanovsky et al., 1997; Yao et al., 2011; Zhuang et al., 2001; Hinzman et al., 1998). However, in this study a simple approach based on the relationship between G and R_N (Eq. (12)) was used to estimate the soil heat flux in the near surface soil layer (around 10 cm depth). This approach has less complexity and requires less input data than the methods mentioned above and allows estimating G at regional scales.

In the Arctic tundra the propagation of the thawing front in the soil active layer consumes a large proportion (around 18%) of the energy input from the positive net radiation (Boike et al., 2008a; Rouse, 1985). Moreover, the presence of permafrost in tundra areas may contribute to the large tundra soil heat flux by creating a strong thermal gradient between the ground surface and depth, offsetting the influence of the highly insulative moss cover which would otherwise have been expected to reduce soil heat flux (Beringer et al., 2005; Blok et al., 2011) (Myers-Smith et al., 2011; Sturm et al., 2001). Therefore, previous formulations of soil heat flux used in TSEB applications, mainly representative of cropped and sparse-vegetated areas, in the U.S., need to be adjusted and validated for Arctic tundra.

~~In past TSEB applications, and according to~~ Currently there are several methodologies that allow estimating soil heat flux from tenths of centimetres to meters in depth in the Arctic tundra by using modelling or instrumentation at several depths (Lynch et al., 1999; Ekici et al., 2015; Jiang et al., 2015; Romanovsky et al., 1997; Yao et al., 2011; Zhuang et al., 2001; Hinzman et al., 1998). However, in this study a simple approach based on the relationship between G and R_{NS} (Eq. (13)) was used to estimate the soil heat flux in the near-surface soil layer (around 10 cm depth). This approach has less complexity and requires less input data than the methods mentioned above and allows estimating G at regional scales.

~~In early TSEB implementation, a constant value of c_G value around 0.3 was used to estimate G for the midmorning to midday period (Eq. (13) based on findings by Kustas and Daughtry (1990) for U.S. study sites. Kustas and Daughtry (1990) and Santanello and Friedl (2003), while a constant value of c_G value around 0.3 can be reasonably used to estimate G for the midmorning to midday period (Eq. (12)). However,~~ this assumption can result in significant errors if applied out of this time range. For diurnal hourly timescales, Kustas et al. (1998), developed a method to estimate c_G based on time differences with the local solar noon quantified by a non-dimensional time parameter, ~~although,~~ Although this approach does not consider the phase shift between G and R_{NS} over a diurnal cycle. ~~However,~~ a phase shift was included in the model proposed by Santanello and Friedl (2003) in the following form:

$$c_G = A \cos[2\pi(t + S)/B], \quad (418)$$

where A represents the maximum value of c_G , B is chosen to minimize the deviation of c_G from Eq. (4213), t is time in seconds relative to solar noon and S is the phase shift between G and R_{NS} in seconds. Values fitted for A , S and B ~~resulted in values of~~ were 0.31, 10 800 and 74 000, respectively.

Although c_G values for Arctic tundra were not found in the literature, several studies present (Beringer et al., 2005; Eugster et al., 2005; Boike et al., 2008b; Eaton et al., 2001; Eugster et al., 2000; Kodama et al., 2007; Langer et al., 2011; Soegaard et al., 2001; Westermann et al., 2009; Mendez et al., 1998; Lund et al., 2014) the relationship between R_{NS} and G during the summer months in similar tundra areas. ~~Based on~~ According to these studies, a mean value of 0.14, as a maximum value of c_G in Eq. (4718), can be derived from different analyses of R_{NS} and G over the Arctic tundra ~~(Beringer et al., 2005; Eugster et al., 2005; Boike et al., 2008b; Eaton et al., 2001; Eugster et al., 2000; Kodama et al., 2007; Langer et al., 2011; Soegaard et al., 2001; Westermann et al., 2009; Mendez et al., 1998; Lund et al., 2014).~~

An alternative parameterization for G suggested by Santanello and Friedl (2003) for several types of soils with crops, and by Jacobsen and Hansen (1999) for Arctic tundra, ~~that~~ links the soil heat flux to the diurnal variations in surface radiometric temperature. This approach can also be applied for Arctic tundra as follows:

$$G = c_{TG} T_{RAD}, \quad (4819)$$

where c_{TG} is a coefficient that represents the relationship between the diurnal variation of T_{RAD} and G . For diurnal hourly timescales, c_{TG} can be also estimated using the phase shift proposed in Eq. (4718); where, in this case, S is the phase shift between G and T_{RAD} in seconds. This new approach avoids using R_{NS} , which is more difficult to define in tundra systems given the influence of the surface ~~organic~~ moss layer above the mineral soil. Moreover, A , S and B in Eq. (4718) can be fitted by using direct measurements of T_{RAD} from thermal field sensors, commonly available on flux towers (pyrgeometer), or thermal data from geostationary or polar satellites.

Thus, to evaluate soil heat flux for diurnal hourly timescales, ~~the approaches of~~ Kustas et al. (1998) and Santanello and Friedl (2003) ~~approaches~~ were compared using the original c_G value of 0.30 and a new value for Arctic tundra of 0.14, ~~both~~ as maximum values of c_G in Eq. (4718). ~~The~~ A , B and S values for the new c_{TG} approach ~~was also~~ were fitted and ~~tested using an extended evaluation dataset and~~ then compared to these radiation-based methods ~~(see section 4.2.4).~~

3.3 Priestley-Taylor coefficient

In the original TSEB formulation, the Priestley-Taylor approach for the canopy component of LE is used. In this case α_{PTC} is normally set to an initial value of 1.26 for the general conditions tested during the growing season in rangelands and croplands. For stressed canopies, TSEB internally modifies α_{PTC} to yield reasonable partitioning between LE_C and LE_S .

As with the c_G coefficient, specific α_{PTC} values for tundra were not found in the literature. Alternatively, measurements of bulk (soil+canopy) for Arctic tundra systems are available (Beringer et al., 2005; Eaton et al., 2001; Eugster et al.,

2005;Engstrom et al., 2002;Mendez et al., 1998;Lund et al., 2014) suggesting a mean value of around 0.92. This bulk value might suggest that α_{PTC} could also be lower for summer Alaska tundra conditions. For natural vegetation, Agam et al. (2010) also suggested that a lower α_{PTC} value might yield better results. Therefore, for modelling purposes two different values of α_{PTC} values, 0.92 and 1.26, were applied to evaluate which nominal α_{PTC} input to TSEB was more appropriate for Arctic
5 tundra.

4 Study area and data description

4.1 Study area

To refine and evaluate the TSEB model for Alaska's Arctic tundra summer conditions, three eddy covariance flux towers (referred to as Fen, Tussock and Heath; see Fig. 1) were selected. These are located across the Innavait Watershed (~904 m
10 a.s.l.) with eddy covariance and associated meteorological data collection beginning in 2007 (Euskirchen et al., 2012; Kade et al., 2012). A brief description of instrumentation at the tower sites is provided in Table 2.

The Fen tower, located at the valley bottom in a wet sedge ecosystem, includes *Eriophorum angustifolium* and dwarf shrubs such as *Betula nana* and *Salix* spp and vegetation types around the tower are comprised of 52% wet sedge, and 47% tussock tundra. The Tussock tower, located at the midslope in a moist acidic tussock tundra ecosystem, is dominated by the tussock-
15 forming sedge *Eriophorum vaginatum*, *Sphagnum* spp., and dwarf shrubs such as *Betula nana* and *Salix* spp. In this case, vegetation types around the flux tower are 95% tussock tundra. The Heath tower sits atop a broad dry ridge at the top edge of the eastern watershed boundary in a heath tundra ecosystem dominated by ~~*Dryas* spp, lichen, and~~ dwarf shrubs and lichen. The vegetation here is 20% heath, but also included 72% tussock tundra, with the balance made of up of sedge meadow and bare soil. Further detailed information about the study is provided in Euskirchen et al. (2012)- and Trochim et al. (2015).

20 4.2 Model inputs and evaluation ~~dataset:~~datasets

4.2.1 Micrometeorological input data ~~and vegetation-based measurements~~

Data incorporated in this study spanned from May to September 2008 to 2012. These included eddy covariance data for latent and sensible collected at 10 Hz and processed to 30-minute means (described below) as well as meteorological data collected at 30-minute intervals (Table 1 and Table 2). These data, from under all sky conditions, were used to refine and
25 evaluate the model performance (Table 1). This dataset was considered to be representative of the short Arctic tundra vegetative cycle from early growing to senescence as well as to capture inter- and intra-annual vegetation dynamics.

Meteorological input for TSEB include wind speed, air temperature, vapour pressure, atmospheric pressure, longwave incoming radiation and solar radiation, all of which were collected at the three measurement sites (see Table 1 and 2). The

surface radiometric temperature T_{RAD} inputs were obtained from the pyrgeometer sensor at the Tussock station and from infrared radiometer sensors at both Fen and Heath stations.

4.2.2 Vegetation properties

In addition, TSEB also requires estimates of LAI and the fraction of vegetation that is green to specify f_C in Eq. (2) and to estimate LE_C in Eq. (10). While, *in situ* measurements of LAI were not available at the tower sites, ~~the for the length of this study, the 500 m combined Terra/Aqua MODIS LAI4-day Leaf Area Index product (MOD15MCD15A3H) was available for the study area. This product has been successfully applied in other applications of the TSEB (Guzinski et al., 2013) where sites are considered homogeneous over several kilometres, and serve here as a proxy for local observations, selecting the best estimates through the LAI product quality flags. The fraction of vegetation that is green (f_C) in Eq. (10) was set equal to the ratio of the fraction of absorbed photosynthetically active radiation (PAR) by the green vegetation and the fraction of PAR intercepted by the total vegetation cover (Guzinski et al., 2013) using the incoming and outgoing PAR from the flux stations. The fraction of vegetation that is green (f_C) in Eq. (10) was estimated using NDVI and EVI from MODIS imagery using the daily 250 m reflectance product (MOD09GQ), and using the blue band in the daily 500 m reflectance product 500 m (MOD09GA) to correct for residual atmospheric effects, with negligible spatial artifacts. Because of MODIS time series contains occasional lower quality data, gaps from persistent clouds, cloud contamination, and other gaps (Gao et al., 2008), a program for analysing time series of remote sensing imagery, TIMESAT (Jönsson and Eklundh, 2004) was used to produce temporally smoothed NDVI, EVI and LAI by selecting the best estimates through these products quality flags. Gao et al. (2008) found a good agreement with field measurements when smoothing MODIS LAI data using this distribution and several weights (w) based on the product quality flags ($w = 1.0$ for LAI retrievals from the radiative-transfer model (high quality) or for LAI retrieval that reaches saturation, $w = 0.25$ for retrievals from an empirical model and $w = 0.0$ for all invalid and fill values). Beck et al. (2006) also reported that an asymmetric Gaussian distribution was appropriate for describing vegetation dynamics using NDVI at high latitudes and several weights (w) based on the product quality flags (highest quality/clear, mixed and cloudy were assigned weights of 1, 0.5 and 0, respectively). For NDVI, EVI and LAI time series smoothing, the weights and quality flags proposed by Beck et al. (2006) and Gao et al. (2008) and were used.~~

Vegetation height, used to define roughness parameters d_0 and z_{OM} , was assigned based on measurements made in the vicinity of the flux towers (Kade et al., 2012) and the clumping factor was set to 1 for all sites based on the knowledge that Arctic tundra has a variable ~~organic moss~~ layer with little bare ground. Variability regarding these inputs for the studied periods is shown in Table 1. Moreover, to ensure that only snow-free periods were analysed, Terra/Aqua MODIS snow cover products (MOD10A1 and MYD10A1) were used to screen days with snow cover at the beginning and end of the growing season. ~~Future work will extend these analyses to periods with snow cover using a snow adapted form of the TSEB (Kongoli et al., 2014).~~

4.2.3 Micrometeorological flux data for model evaluation

The eddy covariance data used in TSEB evaluation, including latent and sensible heat, were processed ~~to account for changes with EddyPro® (2004) software. Changes~~ in mass flow caused by changes in air density (Webb et al., 1980)-
~~Corrections, corrections~~ for frequency attenuation of eddy covariance fluxes following Massman (2000) and Rannik (2001)
5 and storage corrections for calm periods (~~friction velocity (u^*) was less than 0.1 m s^{-1}~~) suggested by Rocha and Shaver (2011)
~~were also applied~~ were accounted for. ~~The automatic gain control (AGC) value (which represents optical impedance by precipitation) was computed for the IRGA and used as a QA/QC variable for both flux and radiation data, with 60 as the maximum threshold value (LI-COR 2004). Rejection angles of 10° were also used when the eddy covariance instruments were downwind of a tower to remove flow distortions. In addition, corrections for stationarity, lags, step-change, among~~
10 ~~others, were performed by the flux processing software~~ (for further information on micrometeorological data processing see Euskirchen et al. (2012)) and http://aon.iab.uaf.edu/data_info). ~~Once the data were processed, they were filtered using quality flag values from the instrumentation to~~ To select the best data available-, ~~the above criteria were used to flag the micrometeorological dataset, and no gap-filled data were used.~~

In addition, soil heat flux plate measurements were corrected to account for soil heat storage above the plate according to the
15 ~~calorimetric methodology of proposed by~~ Domingo et al. (2000) and Lund et al. (2014) using existing field measurements of soil bulk density for each site ($758 \text{ kg}\cdot\text{m}^{-3}$, $989 \text{ kg}\cdot\text{m}^{-3}$ and $1038 \text{ kg}\cdot\text{m}^{-3}$ for Fen, Tussock and Heath flux stations, respectively). ~~The final subset for evaluating the TSEB model was selected by imposing three criteria, identifying periods where), soil moisture from the water content reflectometer and thermocouple averaging soil temperature probes (TCAV) placed at two depths in the soil (see Table 2).~~

To evaluate the new c_{TG} approach, a total of 41068 half-hourly timesteps of T_{RAD} and G from 4 to 21 hours local solar time
20 were selected (11593, 14454 and 15021 for Fen, Tussock and Heath flux stations, respectively). Coefficients A , B and S were fitted using 60% of all available data (fitting subset) aggregated in 30 min timesteps for the whole summer period. The remaining 40% of the data were reserved for model testing (test subset) (see Table 4 for flux stations distribution). To evaluate the TSEB model, including G retrieve from Kustas et al. (1998) and Santanello and Friedl (2003) approaches, a
25 ~~total of 5178 half-hourly timesteps (1558, 1273 and 2347 for Fen, Tussock and Heath flux stations, respectively) was subset from the previous selection by imposing three criteria:~~ a) energy closure at the half-hourly timescale exceeded 70%, b) R_N was higher than $100 \text{ W}\cdot\text{m}^{-2}$ in order to ensure daylight conditions, and c) no precipitation present.

5 Accuracy and error estimation

The performance of the TSEB model and possible refinements for Arctic tundra was evaluated using the coefficient of
30 determination (R^2); the root mean square error (RMSE), the mean bias error (MBE), the mean absolute difference (MAD) and the mean absolute percent difference (MAPD), from Eq. (1920) to Eq. (2324), respectively.

$$R^2 = \left(\frac{\sum_{i=1}^n (o_i - \bar{o})(e_i - \bar{e})}{\sqrt{\sum_{i=1}^n (o_i - \bar{o})^2} \sqrt{\sum_{i=1}^n (e_i - \bar{e})^2}} \right)$$

$$(19) \left(\frac{\sum_{i=1}^n (o_i - \bar{o})(e_i - \bar{e})}{\sqrt{\sum_{i=1}^n (o_i - \bar{o})^2} \sqrt{\sum_{i=1}^n (e_i - \bar{e})^2}} \right), \quad (20)$$

$$RMSE = \sqrt{\frac{\sum_{i=1}^n (e_i - o_i)^2}{n}}, \quad (20)$$

$$MBE = \frac{\sum_{i=1}^n (e_i - o_i)}{n}, \quad (21)$$

$$5 \quad MBE = \frac{\sum_{i=1}^n (e_i - o_i)}{n}, \quad (22)$$

$$MAD = \frac{\sum_{i=1}^n |e_i - o_i|}{n}, \quad (2223)$$

$$MAPD = \frac{100}{\bar{e}} \left(\frac{\sum_{i=1}^n |e_i - o_i|}{n} \right), \quad (2324)$$

where e_i refers to the estimated value of the variable in question (R_N , H, LE or G), o_i is the observed value (*in situ* measurement provided by the flux station), n is the number of data points, and \bar{o} and \bar{e} are the average of the o_i and e_i values, respectively.

6 Results and discussion

6.1 Soil heat flux estimation

Both the Kustas et al., (1998); K98; and the Santanello and Friedl (2003); SF03; soil heat flux models used to estimate G at the study sites yielded high errors when a value of $c_G = 0.3$ was used, with MAPD ranging from 90% to 159%, with%. In this case, the SF03 approach providing provided better results (Table 3). It is important to note that G is a relatively small term with a maximum value on the order of $50 \text{ W}\cdot\text{m}^{-2}$. Both models generally overestimated G with a MBE from $3 \text{ W}\cdot\text{m}^{-2}$ to $40 \text{ W}\cdot\text{m}^{-2}$, with the SF03 model generating lower biases. Results improved when a c_G value of 0.14 was used with MAPD ranging from 48% to 76% and with lower RMSE values from $15 \text{ W}\cdot\text{m}^{-2}$ to $21 \text{ W}\cdot\text{m}^{-2}$ and MBE from $-4 \text{ W}\cdot\text{m}^{-2}$ to $-14 \text{ W}\cdot\text{m}^{-2}$. With the lower value of c_G , the K98 approach provided better results (Table 3).

Similar to the original c_G , c_{TG} can be also estimated using the Santanello and Friedl (2003) method in Eq. (1718). Mean diurnal profiles in T_{RAD} and G, averaged over all tundra study sites, are shown in Fig. (see section 4.2 demonstrating the observed relationships and Table 3) showed a phase shift between these variables (Fig. 2). The mean G value for the summer period peaked around 15:00 local solar time, with a phase shift around 4 hours after the maximum T_{RAD} at noon. Coefficients A, B and S were fitted using 60% of all available data, from 4 to 21 hours local solar time, with no restriction of balance

~~closure, and the remaining 40% of the data were reserved for model testing.~~ Using T_{RAD} and G observations at half-hourly timesteps from the fitting subset, diurnal c_{TG} curves were derived for the growing season for each of the tower sites, showing reasonable agreement (Fig. 3). A fit to the mean curve yielded parameter values of $S = -14\,400$ seconds, $A = 1.55$ and $B = 160\,000$ s. As in the case of Santanello and Friedl (2003), a B variation of $\pm 15\,000$ s had no significant influence on the results. Statistical comparisons between observed fluxes from the test subset and simulations using the fitted parameters show good agreement and negligible bias (Table 4), with R^2 , MAPD, RMSE and MBE values of 0.68, 37%, $6\text{ W}\cdot\text{m}^{-2}$ and $0\text{ W}\cdot\text{m}^{-2}$, respectively. In addition, the new model was also evaluated using the same flux subset used in Table 3 to assess the K98 and SF03 configurations, demonstrating improved performance with roughly half the MAPD than K98 and SF03 configurations (Table 4).

~~To assess typical performance in a remote sensing application this new parameterization should be tested with satellite retrievals of T_{RAD} ; the~~ The performance of the G parameterization for Arctic tundra reported here is comparable or superior to previous studies reported in the literature using the Santanello and Friedl (2003) or Kustas et al. (1998) approaches for other ecosystems. In shrub-grass dominated areas and boreal forest several studies (Anderson et al., 2008; Kustas et al., 1998; Li et al., 2008; Sánchez et al., 2009; Timmermans et al., 2007) reported MAPD and RMSE values ranging from 19% to 59% and from $15\text{ W}\cdot\text{m}^{-2}$ to $35\text{ W}\cdot\text{m}^{-2}$, respectively. Studies in corn and soybean crops (Anderson et al., 2005; Choi et al., 2009; Li et al., 2005; Santanello and Friedl, 2003) reported MAPD and RMSE values ranging from 19% to 34% and from $10\text{ W}\cdot\text{m}^{-2}$ to $41\text{ W}\cdot\text{m}^{-2}$, respectively.

6.2 Net radiation estimation

Effective atmospheric emissivity estimated using the Brutsaert (1975) and Jin et al. (2006) methodologies yielded similar errors in simulated downwelling longwave radiation results, with a R^2 of 0.58 and a RMSE ~~around of $26\text{ W}\cdot\text{m}^{-2}$ and $27\text{ W}\cdot\text{m}^{-2}$, respectively.~~ The C coefficient computed through Jin et al. (2006) yielded a value of 1.25 ± 0.009 , very close to Brutsaert (1975) C value of 1.24. This suggests that the simpler Brutsaert (1975) C coefficient can be used efficiently to model effective atmospheric emissivity in all sky conditions when combined with Crawford and Duchon (1999) and Pons and Ninyerola (2008) methods for summer Arctic tundra.

Estimated R_{N} for all sky condition yielded strong agreement with observed values for all flux towers (see Fig. 4 and Table 5) with a mean R^2 , MAPD, MAD, RMSE of 0.99, 7%, $18\text{ W}\cdot\text{m}^{-2}$, $23\text{ W}\cdot\text{m}^{-2}$, with a tendency to overestimate R_{N} with a MBE of $7\text{ W}\cdot\text{m}^{-2}$. In terms of RMSE and MAPD, all study sites behaved similarly (see Fig. 4). These results are in line with previous TSEB model applications for other cover types and clear sky conditions where a MAPD of around 5% was reported (Anderson et al., 2008; Li et al., 2005; Anderson et al., 2005; Kustas and Norman, 1999; Guzinski et al., 2013; Li et al., 2008; Anderson et al., 2000). This suggest that R_{N} estimation using this ~~methodology~~ scheme can be ~~used to obtain reliable estimates of R_{N} applied regionally~~ under summer all sky conditions in Arctic tundra ~~and can be applied regionally~~ when a

source of solar radiation (METEOSAT or GOES, Cristóbal and Anderson (2013)), air temperature (Cristóbal et al., 2008) and T_{RAD} (MODIS Land Surface Temperature and emissivity product) are available.

6.3 Latent and sensible heat fluxes estimation

The average energy balance closure using half-hour periods for the evaluation ~~subsetdataset~~ was 88% which is in agreement with the average closure of 90% for these flux stations, (Euskirchen et al., 2012). Lack of closure may be explained by instrument and methodological uncertainties, insufficient estimation of storage terms, unmeasured advective fluxes, landscape scale heterogeneity or instrument spatial representativeness, among others (Lund et al., 2014; Stoy et al., 2013; Foken et al., 2011; Foken, 2008; Wilson et al., 2002). While, currently, there is no uniform answer how to deal with non-closure of the energy balance in eddy covariance datasets, and methods for analysing the reasons for the lack of closure are still under discussion (Foken et al., 2011). More recently there is evidence that non-orthogonal sonics underestimate vertical velocity causing under-measurement of H and LE on the order of 10%-% (Kochendorfer et al., 2012; Frank et al., 2013), although this is still being debated (Kochendorfer et al., 2013). In the current study, a distribution of residual according to the Bowen ratio (BR) method was applied as suggested by Twine et al. (2000) and Foken (2008). In addition, LE was recalculated as the residual (RES) of the surface energy budget used in previous TSEB evaluations (Li et al., 2008); and both closure methods were then used to evaluate TSEB output.

Latent (LE) and sensible (H) heat estimated through both the new proposed soil heat flux methodology and the all sky R_N methodology scheme, yielded reasonable agreement with observed data using both closure methods (~~Bowen ratio (BR)~~ and ~~residual (RES)~~) at half-hourly timesteps for both α_{PTC} parameterizations of 0.92 and 1.26 (see Table 5 and 6 and Fig. 4 and 5), although $\alpha_{PTC} = 0.92$ yielded marginally lower errors for the turbulent fluxes of H and LE. Relative errors (MAPD) were ~~3430~~ and ~~2725~~% for LE_{RES} and H, respectively, for all combined sites using $\alpha_{PTC} = 0.92$, and ~~4033~~ and ~~3327~~% using the standard value of $\alpha_{PTC} = 1.26$. Results with LE_{BR} and H_{BR} using $\alpha_{PTC} = 0.92$ yielded MAPD of ~~4235~~ and ~~3630~~%, respectively, while using $\alpha_{PTC} = 1.26$ yielded and ~~4540~~ and ~~4236~~%, respectively.

A slight improvement in H and LE estimates using $\alpha_{PTC} \sim 0.9$ also agrees with Agam et al. (2010) who also found better results with lower α_{PTC} for natural vegetation in water limited environments. Nevertheless, since the mean RMSE for all fluxes and for all parameterizations and sites was around $50 \text{ W}\cdot\text{m}^{-2}$ (Table 5 and 6), which is commensurate with errors typically reported in other surface energy balance studies (Kalma et al., 2008), these results suggest that a generalized α_{PTC} value of 1.26 in global TSEB applications may adequately reproduce energy fluxes in Arctic tundra during the growing season, from leaf-out until senescence, while also capturing inter- and intra-annual dynamics. However, biases in regional applications may be reduced by using a ~~landcover~~land cover class-dependent value of α_{PTC} .

Currently, there is limited research published on application of energy balance models to estimate energy fluxes for Arctic tundra. Mu et al. (2009) reported year-round errors from 20% to 40% in two Arctic tundra sites in Barrow (Alaska, USA) at

5 | daily periods based on a modified aerodynamic resistance–surface energy balance model where the required surface conductance is estimated from remotely-sensed LAI based on Cleugh et al. (2007) formulation. TSEB results, however, were evaluated with half-hourly data in summer conditions and, although they cannot be directly compared with results in this previous study, they show similar errors. As in the case of R_N , LE and H results are also in line with previous works for other cover types using *in situ* data as input to TSEB (Anderson et al., 2000; Anderson et al., 2008; Li et al., 2005).

6.4 Seasonal dynamics of surface energy fluxes and energy partitioning

In general, monthly estimation of surface energy fluxes showed a good agreement with observations during the growing season. Because the model yielded similar results with both α_{PTC} parameterizations of 0.92 and 1.26, this section only shows the seasonal dynamics with α_{PTC} of 0.92. Estimated R_N yielded a low MAPD around 6%, increasing up to 12% at the end of the growing season (Table 7 and Fig. 6). The proposed new method to estimate G yielded better MAPD results from June to August which coincides with the peak of the growing season in July. A similar pattern was found for LE and H, where the best MAPD results occurred also in the middle of the growing season (June and July). MAPD for LE, H and G tended to be higher in May and September; thus coinciding with earlier plant growth or the senesce periods, respectively. ~~MODIS LAI product, used to estimate the fractional vegetation cover to partition soil and canopy temperatures, performed as a good proxy to capture inter- and intra annual vegetation dynamics, performing well for the Arctic tundra and suggesting utility for regional applications (Fig. 7). However, f_G computed using PAR data did not show the same behaviour. While LAI captured seasonal vegetation dynamics, with mean values ranging from 0.7 to 1.7 $m^2 \cdot m^{-2}$, f_G remained almost constant around 0.9, even at the early plant growth or the senesce periods. The presence of a variable organic layer, mainly composed of mosses and lichens that remain green through all the season, might have masked the actual vegetation dynamics (Fig. 7). In addition, mosses may exert strong controls on understory water and heat fluxes in Arctic tundra ecosystems (Blok et al., 2011). The main effect over the model was to overestimate LE and underestimate H, yielding lower agreement with observed data in May and September. Guzinski et al. (2013) suggested a methodology based on EVI and NDVI indices successfully applied to adjust f_G in crops, grasslands and forests; however, further research is needed to apply such methods for the Arctic tundra.~~ MODIS LAI product, used to estimate the fractional vegetation cover (Eq. 3) to partition soil and canopy temperatures, performed as a good proxy to capture inter- and intra-annual vegetation dynamics (Fig. 7). Mean seasonal MODIS LAI from May to September for all flux stations was $1.2 \pm 0.5 m^2 \cdot m^{-2}$. In previous studies close to the study area, Toolik Lake, and Imnaviat Creek (Shaver and Chapin, 1991; Shippert et al., 1995; Williams et al., 2001; Williams et al., 2006) reported LAI field estimates ranging from 0.2 to 1.4 $m^2 \cdot m^{-2}$ for different tundra types around mid-July to mid-August, suggesting LAI overestimation from the MODIS product. Loranty et al. (2010) also reported LAI overestimation when using this product in similar tundra types, finding better agreement using a NDVI-LAI relationship (Shaver et al., 2007; Street et al., 2007), although the nonlinearity in the NDVI-LAI conversion is prone to averaging errors when scaled with remote sensing data (Stoy et al., 2009). Despite MODIS LAI overestimation, it performed well for the Arctic tundra suggesting utility for regional applications, although LAI-NDVI methods might be considered for future applications.

f_G estimated through NDVI and EVI also captured inter- and intra-annual vegetation dynamics (Fig. 7), with a mean seasonal value from May to September for all flux stations of 0.82 ± 0.7 . From May to August (from beginning and almost to the end of the growing period), f_G showed a good agreement with LAI dynamics. However, while f_G showed a steady increase at the beginning of the growing season, it did not follow MODIS LAI dynamics in September. This caused the model to

overestimate LE and underestimate H during this time period, degrading agreement with observed data. The underperformance of the f_G methods near the end of the growing season might be related to the presence of a variable moss layer, which can exert strong controls on understory water and heat fluxes in Arctic tundra ecosystems (Blok et al., 2011) and may have masked the actual vegetation dynamics (Fig. 7). Further research is needed to confirm this hypothesis. The pattern of daily estimated surface energy fluxes also compared well to observed fluxes for all sky conditions. As an example,

time series of modelled and measured surface energy fluxes are segmented in Fig. 8 for the Heath flux station, with each diurnal segment representing flux data averaged by hour over 5-day intervals from 2008 to 2012. Observed and estimated R_N exhibited an excellent agreement showing almost the same daily temporal pattern for the full growing season while LE, H and G yielded a good daily agreement being underestimated in May and September, especially in the case of LE.

In terms of observed (o) and estimated (e) mean season energy flux partitioning, LE_o/R_{No} , H_o/R_{No} and G_o/R_{No} yielded mean values of 0.55, 0.37 and 0.08, respectively; and LE_e/R_{Ne} , H_e/R_{Ne} and G_e/R_{Ne} yielded mean values of 0.58, 0.34 and 0.08, respectively (Fig. 9). Observed and estimated Bowen ratio (β) yielded mean values of 0.5060 and 0.67, respectively. In all cases, observed and estimated results are in line with previous studies in the for Arctic tundra (Lynch et al., 1999; Eugster et al., 2000). It is worth noting that the difference between observed and estimated values of LE/R_N , H/R_N partitions was only around 3% and for G/R_N was almost negligible. From June to August, mean absolute difference values between observed and estimated values for LE/R_N , H/R_N were around 4%, increasing up to 2015% in September due to model over and underestimation, while G/R_N difference was only less than 1%.

These results suggest that the model is able to reproduce accurately temporal trends of energy partition in concert with tundra vegetation dynamics in the growing vegetation peak from June to August and could be used to monitor changes in surface energy fluxes concurrently with vegetation changedynamics.

7 Conclusions and future work

~~An extensive evaluation and refinements in Parameterizations for R_N , G and α_{PTC} parameterizations of a used in the two-source energy balance model (TSEB) to estimate surface energy fluxes in were evaluated and refined for applications in different tundra types in Alaska for over the full Arctic tundra growing season and its interannual dynamics from 2008 to 2012 in all sky conditions was successfully performed. Although there are limited studies that model. Results showed that TSEB may adequately reproduce energy fluxes in Arctic tundra surface energy fluxes, our results compared favourably to these studies conducted at similar sites. A during the growing season, from leaf-out until senescence. The modified TSEB~~

provided turbulent heat flux estimates with a mean RMSE value on the order of $50 \text{ W}\cdot\text{m}^{-2}$ in the turbulent heat fluxes is similar in magnitude to comparison with observations collected at three flux towers – commensurate with errors typically reported in other surface energy balance modelling studies and within the uncertainty in measured fluxes having 80–90% closure studies. The all-sky R_N estimation scheme applied in this work for all sky conditions tested here yielded similar results as errors to those from other studies for only clear sky conditions, showing its. This demonstrates potential for regional scale applications when reliable sources of solar radiation, air temperature and T_{RAD} are available. The new refined model, developed to estimate for soil heat flux (G_s), based on the T_s -soil temperature-G relationship, was validated/evaluated from the early growth/green-up to senescence using data for multiple years (hardly found in the literature); results displayed superior performance yielding, and yielded errors half of the magnitude of the standard TSEB formulation based on the error of other models. Comparable error differences with both relationship between R_{NS} and G . The TSEB α_{PTC} parameterizations of 0.92 and 1.26 were found, suggesting that the original TSEB α_{PTC} of 1.26 for large area modelling is acceptable and valid parameterization for the estimating canopy transpiration (LEc) was tested using the standard TSEB value of 1.26 and a value of 0.92 suggested in the literature for Arctic tundra. However, more research is needed to assess the influence of the organic layer on modelled results. The MODIS LAI product proved to be a reliable input for modelling energy fluxes in Arctic, and both parameterizations yield similar flux errors suggesting tundra in specific values of α_{PTC} are not needed.

In the absence of field data. Results also suggest that in-situ measurements of LAI within the vicinity of the tower sites, the MODIS LAI product provided reasonable inputs for localized model testing. The model is/was able to reproduce accurately temporal trends of energy partitioning in concert with tundra vegetation dynamics in the peak growing season. Moreover, it also has potential to monitor changes in surface energy fluxes in Arctic tundra due to changes in vegetation composition (e.g., shrub encroachment) at regional scales using satellite remote sensing data. This is particularly crucial in the Arctic where there is a sparse network of meteorological and flux observations. Finally, further efforts will be focused on integrate more satellite data to apply. Further research is needed regarding the model to the regional scale the daily energy flux integration by means specific role of the implementation moss layer in modifying remote sensing estimates of green vegetation cover fraction and soil heat conduction within tundra ecosystems.

Future work will incorporate the TSEB model refinements identified here for Arctic tundra into regional and global applications of the ALEXI/DisALEXI surface energy balance modelling system (Anderson et al., 2007; 2011), the dual-temperature difference scheme (Norman et al., 2000; Guzinski et al., 2013), along with data fusion techniques (Cammalleri et al., 2013; 2014) schemes using additional satellite data such as Landsat, Terra/Aqua MODIS or NOAA AVHRR. Model performance within a fully satellite-based remote sensing framework will be compared to the local evaluations reported here at these tundra flux sites. In addition, the diagnostic assessments of ET and surface energy fluxes will be compared with regional output from process-based prognostic land-surface models to better understand the strengths and weaknesses of both types of modelling systems.

Acknowledgements

This research was supported by the Alaska NASA EPSCoR program awards NNX10NO2A and NNX13AB28A. Authors would also like to thank Colin Edgar from the Institute of Arctic Biology, UAF, for his help in data processing of the eddy covariance and meteorological data. Datasets from the Innvait sites were provided by the Institute of Arctic Biology, UAF, based upon work supported by the National Science Foundation under grant #1107892. USDA is an equal opportunity employer and provider.

References

- ~~ACIA: Impacts of a Warming Arctic, Cambridge University Press, Cambridge, 140 pp., 2004.~~
- 10 Agam, N., Kustas, W. P., Anderson, M. C., Norman, J. M., Colaizzi, P. D., Howell, T. A., Prueger, J. H., Meyers, T. P., and Wilson, T. B.: Application of the Priestley–Taylor Approach in a Two-Source Surface Energy Balance Model, *J Hydrometeorol*, 11, 185-198, doi:10.1175/2009jhm1124.1, 2010.
- AMAP: Arctic Climate Issues 2011: Changes in Arctic Snow, Water, Ice and Permafrost. SWIPA 2011. Overview Report, Oslo, Norway, 96 pp., 2012.
- 15 Anderson, M. C., Norman, J. M., Meyers, T. P., and Diak, G. R.: An analytical model for estimating canopy transpiration and carbon assimilation fluxes based on canopy light-use efficiency, *Agr Forest Meteorol*, 101, 265-289, doi:10.1016/S0168-1923(99)00170-7, 2000.
- Anderson, M. C., Norman, J. M., Mecikalski, J. R., Torn, R. D., Kustas, W. P., and Basara, J. B.: A multiscale remote sensing model for disaggregating regional fluxes to micrometeorological scales, *J Hydrometeorol*, 5, 343-363, 2004.
- 20 Anderson, M. C., Norman, J. M., Kustas, W. P., Li, F. Q., Prueger, J. H., and Mecikalski, J. R.: Effects of vegetation clumping on two-source model estimates of surface energy fluxes from an agricultural landscape during SMACEX, *J Hydrometeorol*, 6, 892-909, doi:10.1175/Jhm465.1, 2005.
- Anderson, M. C., Kustas, W. P., and Norman, J. M.: Upscaling Flux Observations from Local to Continental Scales Using Thermal Remote Sensing, *Agron J*, 99, 240, doi:10.2134/agronj2005.0096S, 2007.
- 25 Anderson, M. C., Norman, J., Kustas, W., Houborg, R., Starks, P., and Agam, N.: A thermal-based remote sensing technique for routine mapping of land-surface carbon, water and energy fluxes from field to regional scales, *Remote Sens Environ*, 112, 4227-4241, doi:10.1016/j.rse.2008.07.009, 2008.
- Anderson, M. C., Kustas, W. P., Norman, J. M., Hain, C. R., Mecikalski, J. R., Schultz, L., Gonzalez-Dugo, M. P., Cammalleri, C., d'Urso, G., Pimstein, A., and Gao, F.: Mapping daily evapotranspiration at field to continental scales using geostationary and polar orbiting satellite imagery, *Hydrol Earth Syst Sc*, 15, 223-239, doi:10.5194/hess-15-223-2011, 2011.
- 30

- Anderson, M. C., Kustas, W. P., Alfieri, J. G., Gao, F., Hain, C., Prueger, J. H., Evett, S., Colaizzi, P., Howell, T., and Chávez, J. L.: Mapping daily evapotranspiration at Landsat spatial scales during the BEAREX'08 field campaign, *Advances in Water Resources*, 50, 162-177, doi:10.1016/j.advwatres.2012.06.005, 2012.
- 5 ~~Arendt, A. A., Eichelmeier, K. A., Harrison, W. D., Lingle, C. S., and Valentine, V. B.: Rapid wastage of Alaska glaciers and their contribution to rising sea level, *Science*, 297, 382-386, doi:10.1126/science.1072497, 2002.~~
- Bates, B. C., Kundzewicz, Z. W., S., W., and Palutikof, J. P.: *Climate Change and Water*, Technical Paper of the Intergovernmental Panel on Climate Change, Secretariat, Geneva., 2008.
- Beringer, J., Chapin, F. S., Thompson, C. C., and McGuire, A. D.: Surface energy exchanges along a tundra-forest transition and feedbacks to climate, *Agr Forest Meteorol*, 131, 143-161, doi:10.1016/j.agrformet.2005.05.006, 2005.
- 10 Beck, P. S. A., Atzberger, C., Hogda, K. A., Johansen, B., and Skidmore, A. K.: Improved monitoring of vegetation dynamics at very high latitudes: A new method using MODIS NDVI, *Remote Sens Environ*, 100, 321-334, 10.1016/j.rse.2005.10.021, 2006.
- Bhatt, U. S., Walker, D. A., Raynolds, M. K., Comiso, J. C., Epstein, H. E., Jia, G. S., Gens, R., Pinzon, J. E., Tucker, C. J., Tweedie, C. E., and Webber, P. J.: Circumpolar Arctic Tundra Vegetation Change Is Linked to Sea Ice Decline, *Earth*
- 15 *Interact*, 14, 1-20, Artn 8. doi:10.1175/2010ei315.1, 2010.
- Blok, D., Heijmans, M. M. P. D., Schaepman-Strub, G., van Ruijven, J., Parmentier, F. J. W., Maximov, T. C., and Berendse, F.: The Cooling Capacity of Mosses: Controls on Water and Energy Fluxes in a Siberian Tundra Site, *Ecosystems*, 14, 1055-1065, doi:10.1007/s10021-011-9463-5, 2011.
- Boike, J., Hagedorn, B., and Roth, K.: Heat and Water Transfer Processes in Permafrost Affected Soils: A Review of Field
- 20 and Modeling Based Studies for the Arctic and Antarctic, Plenary Paper, Proceedings of the 9th International Conference on Permafrost, June 29-July 3, 2008, University of Alaska, Fairbanks, USA, 2008a.
- Boike, J., Wille, C., and Abnizova, A.: Climatology and summer energy and water balance of polygonal tundra in the Lena River Delta, Siberia, *J Geophys Res-Biogeophys*, 113, Artn G03025, doi:10.1029/2007jg000540, 2008b.
- Brutsaert, W.: On a derivable formula for long-wave radiation from clear skies, *Water Resour Res*, 11, 742-744,
- 25 doi:10.1029/WR011i005p00742, 1975.
- Cammalleri, C., Anderson, M. C., Ciralo, G., D'Urso, G., Kustas, W. P., La Loggia, G., and Minacapilli, M.: The impact of in-canopy wind profile formulations on heat flux estimation in an open orchard using the remote sensing-based two-source model, *Hydrol Earth Syst Sc*, 14, 2643-2659, doi:10.5194/hess-14-2643-2010, 2010.
- Cammalleri, C., Anderson, M. C., Ciralo, G., D'Urso, G., Kustas, W. P., La Loggia, G., and Minacapilli, M.: Applications
- 30 of a remote sensing-based two-source energy balance algorithm for mapping surface fluxes without in situ air temperature observations, *Remote Sens Environ*, 124, 502-515, doi:10.1016/j.rse.2012.06.009, 2012.
- Cammalleri, C., Anderson, M. C., Gao, F., Hain, C. R., and Kustas, W. P.: A data fusion approach for mapping daily evapotranspiration at field scale, *Water Resour Res*, 49, 4672-4686, doi:10.1002/wrcr.20349, 2013.

- Cammalleri, C., Anderson, M. C., Gao, F., Hain, C. R., and Kustas, W. P.: Mapping daily evapotranspiration at field scales over rainfed and irrigated agricultural areas using remote sensing data fusion, *Agr Forest Meteorol*, 186, 1-11, doi:10.1016/j.agrformet.2013.11.001, 2014.
- Choi, M., Kustas, W. P., Anderson, M. C., Allen, R. G., Li, F., and Kjaersgaard, J. H.: An intercomparison of three remote sensing-based surface energy balance algorithms over a corn and soybean production region (Iowa, U.S.) during SMACEX, *Agr Forest Meteorol*, 149, 2082-2097, doi:10.1016/j.agrformet.2009.07.002, 2009.
- Cleugh, H. A., Leuning, R., Mu, Q. Z., and Running, S. W.: Regional evaporation estimates from flux tower and MODIS satellite data, *Remote Sens Environ*, 106, 285-304, doi:10.1016/j.rse.2006.07.007, 2007.
- Crawford, T. M., and Duchon, C. E.: An improved parameterization for estimating effective atmospheric emissivity for use in calculating daytime downwelling longwave radiation, *J Appl Meteorol*, 38, 474-480, doi:10.1175/1520-0450;2, 1999.
- Cristóbal, J., Ninyerola, M., and Pons, X.: Modeling air temperature through a combination of remote sensing and GIS data, *Journal of Geophysical Research*, 113, 1-13, doi:10.1029/2007jd009318, 2008.
- Cristóbal, J., and Anderson, M. C.: Validation of a Meteosat Second Generation solar radiation dataset over the northeastern Iberian Peninsula, *Hydrol Earth Syst Sc*, 17, 163-175, doi:10.5194/hess-17-163-2013, 2013.
- Daughtry, C. S. T., Kustas, W. P., Moran, M. S., Pinter, P. J., Jackson, R. D., Brown, P. W., Nichols, W. D., and Gay, L. W.: Spectral Estimates of Net-Radiation and Soil Heat-Flux, *Remote Sens Environ*, 32, 111-124, doi:10.1016/0034-4257(90)90012-B, 1990.
- Deardorff, J. W.: Efficient prediction of ground surface temperature and moisture, with inclusion of a layer of vegetation, *Journal of Geophysical Research*, 83, 1889, doi:10.1029/JC083iC04p01889, 1978.
- Domingo, F., Villagarcia, L., Brenner, A. J., and Puigdefabregas, J.: Measuring and modelling the radiation balance of a heterogeneous shrubland, *Plant Cell Environ*, 23, 27-38, doi:10.1046/j.1365-3040.2000.00532.x, 2000.
- Eaton, A. K., Rouse, W. R., Lafleur, P. M., Marsh, P., and Blanken, P. D.: Surface energy balance of the western and central Canadian subarctic: Variations in the energy balance among five major terrain types, *J Climate*, 14, 3692-3703, doi:10.1175/1520-0442, 2001.
- [Duursma, R. A., and Medlyn, B. E.: MAESPA: a model to study interactions between water limitation, environmental drivers and vegetation function at tree and stand levels, with an example application to CO₂ × drought interactions, *Geoscientific Model Development*, 5, 919-940, 10.5194/gmd-5-919-2012, 2012.](#)
- [Ek, M. B., Mitchell, K. E., Lin, Y., Rogers, E., Grunmann, P., Koren, V., Gayno, G., and Tarpley, J. D.: Implementation of Noah land surface model advances in the National Centers for Environmental Prediction operational mesoscale Eta model, *J Geophys Res-Atmos*, 108, n/a-n/a, Artn 885110.1029/2002jd003296, 2003.](#)
- Ekici, A., Chadburn, S., Chaudhary, N., Hajdu, L. H., Marmy, A., Peng, S., Boike, J., Burke, E., Friend, A. D., Hauck, C., Krinner, G., Langer, M., Miller, P. A., and Beer, C.: Site-level model intercomparison of high latitude and high altitude soil thermal dynamics in tundra and barren landscapes, *Cryosphere*, 9, 1343-1361, doi:10.5194/tc-9-1343-2015, 2015.

- Elmendorf, S. C., Henry, G. H. R., Hollister, R. D., Bjork, R. G., Boulanger-Lapointe, N., Cooper, E. J., Cornelissen, J. H. C., Day, T. A., Dorrepaal, E., Elumeeva, T. G., Gill, M., Gould, W. A., Harte, J., Hik, D. S., Hofgaard, A., Johnson, D. R., Johnstone, J. F., Jonsdottir, I. S., Jorgenson, J. C., Klanderud, K., Klein, J. A., Koh, S., Kudo, G., Lara, M., Levesque, E., Magnusson, B., May, J. L., Mercado-Diaz, J. A., Michelsen, A., Molau, U., Myers-Smith, I. H., Oberbauer, S. F., Onipchenko, V. G., Rixen, C., Schmidt, N. M., Shaver, G. R., Spasojevic, M. J., Porhallsdottir, P. E., Tolvanen, A., Troxler, T., Tweedie, C. E., Villareal, S., Wahren, C. H., Walker, X., Webber, P. J., Welker, J. M., and Wipf, S.: Plot-scale evidence of tundra vegetation change and links to recent summer warming, *Nat Clim Change*, 2, 453-457, doi:10.1038/Nclimate1465, 2012.
- 5 [EddyPro® \(Version 5\) \[Computer software\]. 2014. Lincoln, NE. LI-COR, Inc; Infrastructure for Measurements of the European Carbon Cycle consortium.](#)
- 10 Engstrom, R. N., Hope, A. S., Stow, D. A., Vourlitis, G. L., and Oechel, W. C.: Priestley-Taylor Alpha Coefficient: Variability and Relationship to Ndvi in Arctic Tundra Landscapes, *J Am Water Resour As*, 38, 1647-1659, doi:10.1111/j.1752-1688, 2002.
- Eugster, W., Rouse, W. R., Pielke, R. A., McFadden, J. P., Baldocchi, D. D., Kittel, T. G. F., Chapin, F. S., Liston, G. E., Vidale, P. L., Vaganov, E., and Chambers, S.: Land-atmosphere energy exchange in Arctic tundra and boreal forest: available data and feedbacks to climate, *Global Change Biol*, 6, 84-115, doi:10.1046/j.1365-2486, 2000.
- 15 Eugster, W., McFadden, J. P., and Chapin, F. S.: Differences in Surface Roughness, Energy, and CO₂ Fluxes in Two Moist Tundra Vegetation Types, Kuparuk Watershed, Alaska, U.S.A., 2005.
- Euskirchen, E. S., Bret-Harte, M. S., Scott, G. J., Edgar, C., and Shaver, G. R.: Seasonal patterns of carbon dioxide and water fluxes in three representative tundra ecosystems in northern Alaska, *Ecosphere*, 3, art4, 10.1890/es11-00202.1, 2012.
- 20 [Falge, E., Reth, S., Bruggemann, N., Butterbach-Bahl, K., Goldberg, V., Oltchev, A., Schaaf, S., Spindler, G., Stiller, B., Queck, R., Kostner, B., and Bernhofer, C.: Comparison of surface energy exchange models with eddy flux data in forest and grassland ecosystems of Germany. *Ecol Model*, 188, 174-216, 10.1016/j.ecolmodel.2005.01.057, 2005.](#)
- Foken, T.: The energy balance closure problem: an overview, *Ecol Appl*, 18, 1351-1367, doi:10.1890/06-0922.1, 2008.
- 25 Foken, T., Aubinet, M., Finnigan, J. J., Leclerc, M. Y., Mauder, M., and U, K. T. P.: Results of a Panel Discussion About the Energy Balance Closure Correction for Trace Gases, *B Am Meteorol Soc*, 92, Es13-Es18, doi:10.1175/2011BAMS3130.1, 2011.
- Frank, J. M., Massman, W. J., and Ewers, B. E.: Underestimates of sensible heat flux due to vertical velocity measurement errors in non-orthogonal sonic anemometers, *Agr Forest Meteorol*, 171, 72-81, doi:10.1016/j.agrformet.2012.11.005, 2013.
- 30 [Fisher, J. B., Tu, K. P., and Baldocchi, D. D.: Global estimates of the land-atmosphere water flux based on monthly AVHRR and ISLSCP-II data, validated at 16 FLUXNET sites, *Remote Sens Environ*, 112, 901-919, doi:10.1016/j.rse.2007.06.025, 2008.](#)

[Gao, F., Morisette, J. T., Wolfe, R. E., Ederer, G., Pedelty, J., Masuoka, E., Myneni, R., Tan, B., and Nightingale, J.: An algorithm to produce temporally and spatially continuous MODIS-LAI time series, *Ieee Geosci Remote S*, 5, 60-64, 10.1109/Lgrs.2007.907971, 2008.](#)

Guzinski, R., Anderson, M. C., Kustas, W. P., Nieto, H., and Sandholt, I.: Using a thermal-based two source energy balance model with time-differencing to estimate surface energy fluxes with day–night MODIS observations, *Hydrol Earth Syst Sc*, 17, 2809-2825, doi:10.5194/hess-17-2809-2013, 2013.

[Hain, C. R., Crow, W. T., Anderson, M. C., and Yilmaz, M. T.: Diagnosing Neglected Soil Moisture Source-Sink Processes via a Thermal Infrared-Based Two-Source Energy Balance Model, *J Hydrometeorol*, 16, 1070-1086, 10.1175/Jhm-D-14-0017.1, 2015.](#)

[Haverd, V., Raupach, M. R., Briggs, P. R., Canadell, J. G., Isaac, P., Pickett-Heaps, C., Roxburgh, S. H., van Gorsel, E., Viscarra Rossel, R. A., and Wang, Z.: Multiple observation types reduce uncertainty in Australia's terrestrial carbon and water cycles, *Biogeosciences*, 10, 2011-2040, 10.5194/bg-10-2011-2013, 2013.](#)

Hinzman, L. D., Goering, D. J., and Kane, D. L.: A distributed thermal model for calculating soil temperature profiles and depth of thaw in permafrost regions, *J Geophys Res-Atmos*, 103, 28975-28991, doi:10.1029/98jd01731, 1998.

Jacobsen, A., and Hansen, B. U.: Estimation of the soil heat flux net radiation ratio based on spectral vegetation indexes in high-latitude Arctic areas, *Int J Remote Sens*, 20, 445-461, doi:10.1080/014311699213532, 1999.

Jia, G. J., Epstein, H. E., and Walker, D. A.: Greening of arctic Alaska, 1981–2001, *Geophys Res Lett*, 30, 2067, doi:10.1029/2003gl018268, 2003.

Jiang, Y. Y., Rocha, A. V., O'Donnell, J. A., Drysdale, J. A., Rastetter, E. B., Shaver, G. R., and Zhuang, Q. L.: Contrasting soil thermal responses to fire in Alaskan tundra and boreal forest, *J Geophys Res-Earth*, 120, 363-378, doi:10.1002/2014JF003180, 2015.

Jin, X., Barber, D., and Papakyriakou, T.: A new clear-sky downward longwave radiative flux parameterization for Arctic areas based on rawinsonde data, *J Geophys Res-Atmos*, 111, Artn D24104. doi:10.1029/2005jd007039, 2006.

Jung, M., Reichstein, M., Ciais, P., Seneviratne, S. I., Sheffield, J., Goulden, M. L., Bonan, G., Cescatti, A., Chen, J., de Jeu, R., Dolman, A. J., Eugster, W., Gerten, D., Gianelle, D., Gobron, N., Heinke, J., Kimball, J., Law, B. E., Montagnani, L., Mu, Q., Mueller, B., Oleson, K., Papale, D., Richardson, A. D., Rouspard, O., Running, S., Tomelleri, E., Viovy, N., Weber, U., Williams, C., Wood, E., Zaehle, S., and Zhang, K.: Recent decline in the global land evapotranspiration trend due to limited moisture supply, *Nature*, 467, 951-954, doi:10.1038/nature09396, 2010.

[Jönsson, P., and Eklundh, L.: TIMESAT—a program for analyzing time-series of satellite sensor data, *Comput Geosci-Uk*, 30, 833-845, 10.1016/j.cageo.2004.05.006, 2004.](#)

Kade, A., Bret-Harte, M. S., Euskirchen, E. S., Edgar, C., and Fulweber, R. A.: Upscaling of CO₂ fluxes from heterogeneous tundra plant communities in Arctic Alaska, *Journal of Geophysical Research*, 117, doi:10.1029/2012jg002065, 2012.

Kalma, J. D., McVicar, T. R., and McCabe, M. F.: Estimating Land Surface Evaporation: A Review of Methods Using Remotely Sensed Surface Temperature Data, *Surv Geophys*, 29, 421-469, doi:10.1007/s10712-008-9037-z, 2008.

- Kane, D. L., Gieck, R. E., and Hinzman, L. D.: Evapotranspiration from a Small Alaskan Arctic Watershed, *Nordic Hydrology*, 21, 253-272, 1990.
- Kane, D. L., Gieck, R. E., Kitover, D. C., Hinzman, L. D., Mcnamara, J. P., and Yang, D.: Hydrologic Cycle on the North Slope of Alaska, 2004.
- 5 Kane, D. L., and Yang, D.: Overview for Water Balance Determinations for High Latitude Watersheds, 2004.
- Kodama, Y., Sato, N., Yabuki, H., Ishii, Y., Nomura, M., and Ohata, T.: Wind direction dependency of water and energy fluxes and synoptic conditions over a tundra near Tiksi, Siberia, *Hydrol Process*, 21, 2028-2037, doi:10.1002/hyp.6712, 2007.
- Kongoli, C., Kustas, W. P., Anderson, M. C., Norman, J. M., Alfieri, J. G., Flerchinger, G. N., and Marks, D.: Evaluation of a Two-Source Snow–Vegetation Energy Balance Model for Estimating Surface Energy Fluxes in a Rangeland Ecosystem, *J Hydrometeorol*, 15, 143-158, doi:10.1175/jhm-d-12-0153.1, 2014.
- 10 Kustas, W. P., and Daughtry, C. S. T.: Estimation of the Soil Heat-Flux Net-Radiation Ratio from Spectral Data, *Agr Forest Meteorol*, 49, 205-223, doi:10.1016/0168-1923(90)90033-3, 1990.
- Kustas, W. P., Zhan, X., and Schmugge, T. J.: Combining optical and microwave remote sensing for mapping energy fluxes in a semiarid watershed, *Remote Sens Environ*, 64, 116-131, doi:10.1016/S0034-4257(97)00176-4, 1998.
- 15 Kustas, W. P., and Norman, J. M.: Evaluation of soil and vegetation heat flux predictions using a simple two-source model with radiometric temperatures for partial canopy cover, *Agr Forest Meteorol*, 94, 13-29, doi:10.1016/S0168-1923(99)00005-2, 1999.
- Kustas, W. P., and Norman, J. M.: A two-source energy balance approach using directional radiometric temperature observations for sparse canopy covered surfaces, *Agron J*, 92, 847-854, 2000.
- 20 Kochendorfer, J., Meyers, T. P., Frank, J., Massman, W. J., and Heuer, M. W.: How Well Can We Measure the Vertical Wind Speed? Implications for Fluxes of Energy and Mass, *Bound-Lay Meteorol*, 145, 383-398, doi:10.1007/s10546-012-9738-1, 2012.
- Kochendorfer, J., Meyers, T. P., Frank, J. M., Massman, W. J., and Heuer, M. W.: Reply to the Comment by Mauder on “How Well Can We Measure the Vertical Wind Speed? Implications for Fluxes of Energy and Mass”, *Bound-Lay Meteorol*, 147, 337-345, doi:10.1007/s10546-012-9792-8, 2012.
- 25 ~~Lammers, R. B., Shiklomanov, A. I., Vorosmarty, C. J., Fekete, B. M., and Peterson, B. J.: Assessment of contemporary Arctic river runoff based on observational discharge records, *J Geophys Res Atmos*, 106, 3321-3334, doi:10.1029/2000jd900444, 2001.~~
- 30 Langer, M., Westermann, S., Muster, S., Piel, K., and Boike, J.: The surface energy balance of a polygonal tundra site in northern Siberia - Part 1: Spring to fall, *Cryosphere*, 5, 151-171, doi:10.5194/tc-5-151-2011, 2011.
- Li, F., Kustas, W. P., Anderson, M. C., Prueger, J. H., and Scott, R. L.: Effect of remote sensing spatial resolution on interpreting tower-based flux observations, *Remote Sens Environ*, 112, 337-349, doi:10.1016/j.rse.2006.11.032, 2008.

- Li, F. Q., Kustas, W. P., Prueger, J. H., Neale, C. M. U., and Jackson, T. J.: Utility of remote sensing-based two-source energy balance model under low- and high-vegetation cover conditions, *J Hydrometeorol*, 6, 878-891, doi:10.1175/Jhm464.1, 2005.
- [LI-COR Inc. LI-7500 CO2/H2O analyzer instruction manual. LI-COR, Lincoln, Nebraska, USA, 2004.](#)
- 5 [Lorant, M. M., Goetz, S. J., Rastetter, E. B., Rocha, A. V., Shaver, G. R., Humphreys, E. R., and Lafleur, P. M.: Scaling an Instantaneous Model of Tundra NEE to the Arctic Landscape. *Ecosystems*, 14, 76-93, doi:10.1007/s10021-010-9396-4, 2010.](#)
- Lund, M., Hansen, B. U., Pedersen, S. H., Stiegler, C., and Tamstorf, M. P.: Characteristics of summer-time energy exchange in a high Arctic tundra heath 2000-2010, *Tellus B*, 66, doi:10.3402/Tellusb.V66.21631, 2014.
- 10 Lynch, A. H., Chapin, F. S., Hinzman, L. D., Wu, W., Lilly, E., Vourlitis, G., and Kim, E.: Surface energy balance on the arctic tundra: Measurements and models, *J Climate*, 12, 2585-2606, doi:10.1175/1520-0442;2, 1999.
- Massman, W. J.: A simple method for estimating frequency response corrections for eddy covariance systems, *Agr Forest Meteorol*, 104, 185-198, doi:10.1016/S0168-1923(00)00164-7, 2000.
- Mendez, J., Hinzman, L. D., and Kane, D. L.: Evapotranspiration from a wetland complex on the Arctic coastal plain of
15 Alaska, *Nordic Hydrology*, 29, 303-330, 1998.
- Mu, Q. Z., Jones, L. A., Kimball, J. S., McDonald, K. C., and Running, S. W.: Satellite assessment of land surface evapotranspiration for the pan-Arctic domain, *Water Resour Res*, 45, Artn W09420 doi:10.1029/2008wr007189, 2009.
- Myers-Smith, I. H., Forbes, B. C., Wilking, M., Hallinger, M., Lantz, T., Blok, D., Tape, K. D., Macias-Fauria, M., Sass-Klaassen, U., Levesque, E., Boudreau, S., Ropars, P., Hermanutz, L., Trant, A., Collier, L. S., Weijers, S., Rozema, J.,
20 Rayback, S. A., Schmidt, N. M., Schaeppman-Strub, G., Wipf, S., Rixen, C., Menard, C. B., Venn, S., Goetz, S., Andreu-Hayles, L., Elmendorf, S., Ravolainen, V., Welker, J., Grogan, P., Epstein, H. E., and Hik, D. S.: Shrub expansion in tundra ecosystems: dynamics, impacts and research priorities, *Environmental Research Letters*, 6, doi:10.1088/1748-9326/6/4/045509, 2011.
- Norman, J. M., Kustas, W. P., and Humes, K. S.: Source Approach for Estimating Soil and Vegetation Energy Fluxes in
25 Observations of Directional Radiometric Surface-Temperature, *Agr Forest Meteorol*, 77, 263-293, doi:10.1016/0168-1923(95)02265-Y, 1995.
- Norman, J. M., Kustas, W. P., Prueger, J. H., and Diak, G. R.: Surface flux estimation using radiometric temperature: A dual-temperature-difference method to minimize measurement errors, *Water Resour Res*, 36, 2263, doi:10.1029/2000wr900033, 2000.
- 30 Overduin, P. P., and Kane, D. L.: Frost boils and soil ice content: Field observations, *Permafrost Periglac*, 17, 291-307, Doi 10.1002/Ppp.567, 2006.
- Pons, X., and Ninyerola, M.: Mapping a topographic global solar radiation model implemented in a GIS and refined with ground data, *Int J Climatol*, 28, 1821-1834, doi:10.1002/Joc.1676, 2008.

- Priestley, C. H. B., and Taylor, R. J.: On the assessment of surface heat flux and evaporation using large-scale parameters, *Mon Weather Rev*, 100, 81-92, 1972.
- Rannik, Ü.: A comment on the paper by W.J. Massman 'A simple method for estimating frequency response corrections for eddy covariance systems', *Agr Forest Meteorol*, 107, 241-245, [http://dx.doi.org/10.1016/S0168-1923\(00\)00236-7](http://dx.doi.org/10.1016/S0168-1923(00)00236-7), 2001.
- 5 Rawlins, M. A., Steele, M., Holland, M. M., Adam, J. C., Cherry, J. E., Francis, J. A., Groisman, P. Y., Hinzman, L. D., Huntington, T. G., Kane, D. L., Kimball, J. S., Kwok, R., Lammers, R. B., Lee, C. M., Lettenmaier, D. P., McDonald, K. C., Podest, E., Pundsack, J. W., Rudels, B., Serreze, M. C., Shiklomanov, A., Skagseth, O., Troy, T. J., Vorosmarty, C. J., Wensnahan, M., Wood, E. F., Woodgate, R., Yang, D. Q., Zhang, K., and Zhang, T. J.: Analysis of the Arctic System for Freshwater Cycle Intensification: Observations and Expectations, *J Climate*, 23, 5715-5737, doi:10.1175/2010jcli3421.1,
- 10 2010.
- Rocha, A. V., and Shaver, G. R.: Burn severity influences postfire CO₂ exchange in arctic tundra, *Ecol Appl*, 21, 477-489, doi:10.1890/10-0255.1, 2011.
- Romanovsky, V. E., Osterkamp, T. E., and Duxbury, N. S.: An evaluation of three numerical models used in simulations of the active layer and permafrost temperature regimes, *Cold Reg Sci Technol*, 26, 195-203, doi:10.1016/S0165-
- 15 232x(97)00016-5, 1997.
- Rouse, W. R.: Microclimate of Arctic Tree Line .2. Soil Microclimate of Tundra and Forest, *Water Resour Res*, 20, 67-73, doi:10.1029/Wr020i001p00067, 1984.
- Sánchez, J. M., Caselles, V., Niclòs, R., Coll, C., and Kustas, W. P.: Estimating energy balance fluxes above a boreal forest from radiometric temperature observations, *Agr Forest Meteorol*, 149, 1037-1049, 10.1016/j.agrformet.2008.12.009, 2009.
- 20 Santanello, J. A., and Friedl, M. A.: Diurnal covariation in soil heat flux and net radiation, *J Appl Meteorol*, 42, 851-862, 2003.
- Serreze, M. C., and Barry, R. G.: Processes and impacts of Arctic amplification: A research synthesis, *Global Planet Change*, 77, 85-96, doi:10.1016/j.gloplacha.2011.03.004, 2011.
- [Shaver, G. R., and Chapin, F. S.: Production - Biomass Relationships and Element Cycling in Contrasting Arctic Vegetation Types, *Ecol Monogr*, 61, 1-31, doi:10.2307/1942997, 1991.](#)
- 25 [Shaver, G. R., Street, L. E., Rastetter, E. B., Van Wijk, M. T., and Williams, M.: Functional convergence in regulation of net CO₂ flux in heterogeneous tundra landscapes in Alaska and Sweden, *J Ecol*, 95, 802-817, doi:10.1111/j.1365-2745.2007.01259.x, 2007.](#)
- [Shippert, M. M., Walker, D. A., Auerbach, N. A., and Lewis, B. R.: Biomass and leaf-area index maps derived from SPOT images for Toolik Lake and Imnavait Creek areas, Alaska, *Polar Record*, 31, 147-154, 1995.](#)
- 30 Shutov, V., Gieck, R. E., Hinzman, L. D., and Kane, D. L.: Evaporation from land surface in high latitude areas: a review of methods and study results, *Nordic Hydrology*, 37, 393-411, doi:10.2166/Nh.2006.022, 2006.

[Smith, B., Prentice, I. C., and Sykes, M. T.: Representation of vegetation dynamics in the modelling of terrestrial ecosystems: comparing two contrasting approaches within European climate space, *Global Ecol Biogeogr*, 10, 621-637, DOI 10.1046/j.1466-822X.2001.t01-1-00256.x, 2001.](#)

5 Soegaard, H., Hasholt, B., Friberg, T., and Nordstroem, C.: Surface energy- and water balance in a high-arctic environment in NE Greenland, *Theor Appl Climatol*, 70, 35-51, doi:10.1007/s007040170004, 2001.

Stoy, P. C., Mauder, M., Foken, T., Marcolla, B., Boegh, E., Ibrom, A., Arain, M. A., Arneth, A., Aurela, M., Bernhofer, C., Cescatti, A., Dellwik, E., Duce, P., Gianelle, D., van Gorsel, E., Kiely, G., Knohl, A., Margolis, H., McCaughey, H., Merbold, L., Montagnani, L., Papale, D., Reichstein, M., Saunders, M., Serrano-Ortiz, P., Sottocornola, M., Spano, D., Vaccari, F., and Varlagin, A.: A data-driven analysis of energy balance closure across FLUXNET research sites: The role of
10 landscape scale heterogeneity, *Agr Forest Meteorol*, 171, 137-152, doi:10.1016/j.agrformet.2012.11.004, 2013.

Sturm, M., Racine, C., and Tape, K.: Climate change. Increasing shrub abundance in the Arctic, *Nature*, 411, 546-547, doi:10.1038/35079180, 2001.

15 [Stoy, P. C., Williams, M., Spadavecchia, L., Bell, R. A., Prieto-Blanco, A., Evans, J. G., and van Wijk, M. T.: Using Information Theory to Determine Optimum Pixel Size and Shape for Ecological Studies: Aggregating Land Surface Characteristics in Arctic Ecosystems, *Ecosystems*, 12, 574-589, 10.1007/s10021-009-9243-7, 2009.](#)

[Street, L. E., Shaver, G. R., Williams, M., and Van Wijk, M. T.: What is the relationship between changes in canopy leaf area and changes in photosynthetic CO₂ flux in arctic ecosystems?, *J Ecol*, 95, 139-150, doi:10.1111/j.1365-2745.2006.01187.x, 2007.](#)

20 [Tang, R. L., Li, Z. L., Jia, Y. Y., Li, C. R., Sun, X. M., Kustas, W. P., and Anderson, M. C.: An intercomparison of three remote sensing-based energy balance models using Large Aperture Scintillometer measurements over a wheat-corn production region, *Remote Sens Environ*, 115, 3187-3202, 10.1016/j.rse.2011.07.004, 2011.](#)

Tanner, C. B., and Jury, W. A.: Estimating evaporation and transpiration from a row crop during incomplete cover, *Agron. J.*, 68, 239-242, 1976.

25 Timmermans, W. J., Kustas, W. P., Anderson, M. C., and French, A. N.: An intercomparison of the Surface Energy Balance Algorithm for Land (SEBAL) and the Two-Source Energy Balance (TSEB) modeling schemes, *Remote Sens Environ*, 108, 369-384, doi:10.1016/j.rse.2006.11.028, 2007.

[Twine, T., Trochim, E. D., Jorgenson, M. T., Prakash, A., and Kane, D. L.: Geomorphic and biophysical factors affecting water tracks in northern Alaska, *Earth and Space Science*, 3, 123-141, 10.1002/2015ea000111, 2016.](#)

30 [Twine, T. E., Kustas, W. P., Norman, J. M., Cook, D. R., Houser, P. R., Meyers, T. P., Prueger, J. H., Starks, P. J., and Wesely, M. L.: Correcting eddy-covariance flux underestimates over a grassland, *Agr Forest Meteorol*, 103, 279-300, doi:10.1016/S0168-1923\(00\)00123-4, 2000.](#)

[Vinukollu, R. K., Sheffield, J., Wood, E. F., Bosilovich, M. G., and Mocko, D.: Multimodel Analysis of Energy and Water Fluxes: Intercomparisons between Operational Analyses, a Land Surface Model, and Remote Sensing, *J Hydrometeorol*, 13, 3-26, 10.1175/2011JHM1372.1, 2012.](#)

- Vörösmarty, C. J., Hinzman, L. D., Peterson, B. J., Bromwich, D. H., Hamilton, L. C., Morison, J., Romanovsky, V. E., Sturm, M., and Webb, R. S.: The Hydrologic Cycle and its Role in Arctic and Global Environmental Change: A Rationale and Strategy for Synthesis Study, Fairbanks, Alaska, 84 pp., 2001.
- Webb, E. K., Pearman, G. I., and Leuning, R.: Correction of Flux Measurements for Density Effects Due to Heat and Water-
5 Vapor Transfer, *Q J Roy Meteor Soc*, 106, 85-100, doi:10.1002/qj.49710644707, 1980.
- Westermann, S., Luers, J., Langer, M., Piel, K., and Boike, J.: The annual surface energy budget of a high-arctic permafrost site on Svalbard, Norway, *Cryosphere*, 3, 245-263, 2009.
- Wilson, K., Goldstein, A., Falge, E., Aubinet, M., Baldocchi, D., Berbigier, P., Bernhofer, C., Ceulemans, R., Dolman, H., Field, C., Grelle, A., Ibrom, A., Law, B. E., Kowalski, A., Meyers, T., Moncrieff, J., Monson, R., Oechel, W., Tenhunen, J.,
10 [Williams, M., Rastetter, E. B., Shaver, G. R., Hobbie, J. E., Carpino, E., and Kwiatkowski, B. L.: Primary production of an arctic watershed: An uncertainty analysis, *Ecol Appl*, 11, doi:1800-1816, 10.1890/1051-0761, 2001.](#)
- [Williams, M., Street, L. E., van Wijk, M. T., and Shaver, G. R.: Identifying differences in carbon exchange among arctic ecosystem types, *Ecosystems*, 9, 288-304, doi:10.1007/s10021-005-0146-y, 2006.](#)
- [Williamson, S. N., Barrio, I. C., Hik, D. S., and Gamon, J. A.: Phenology and species determine growing-season albedo
15 \[increase at the altitudinal limit of shrub growth in the sub-Arctic, *Glob Chang Biol*, 1-11, 10.1111/gcb.13297, 2016.\]\(#\)](#)
- Valentini, R., and Verma, S.: Energy balance closure at FLUXNET sites, *Agr Forest Meteorol*, 113, 223-243, 2002.
- Xu, L., Myneni, R. B., Chapin, F. S., Callaghan, T. V., Pinzon, J. E., Tucker, C. J., Zhu, Z., Bi, J., Ciais, P., Tommervik, H., Euskirchen, E. S., Forbes, B. C., Piao, S. L., Anderson, B. T., Ganguly, S., Nemani, R. R., Goetz, S. J., Beck, P. S. A., Bunn, A. G., Cao, C., and Stroeve, J. C.: Temperature and vegetation seasonality diminishment over northern lands, *Nat Clim
20 Change*, 3, 581-586, doi:10.1038/Nclimate1836, 2013.
- Yao, J. M., Zhao, L., Gu, L. L., Qiao, Y. P., and Jiao, K. Q.: The surface energy budget in the permafrost region of the Tibetan Plateau, *Atmos Res*, 102, 394-407, doi:10.1016/j.atmosres.2011.09.001, 2011.
- Zhang, K., Kimball, J. S., Nemani, R. R., and Running, S. W.: A continuous satellite-derived global record of land surface evapotranspiration from 1983 to 2006, *Water Resour Res*, 46, Artn W09522, doi:10.1029/2009wr008800, 2010.
- 25 Zhang, Z., Kane, D. L., and Hinzman, L. D.: Development and application of a spatially-distributed Arctic hydrological and thermal process model (ARHYTHM), *Hydrol Process*, 14, 1017-1044, 2000.
- Zhuang, Q., Romanovsky, V. E., and McGuire, A. D.: Incorporation of a permafrost model into a large-scale ecosystem model: Evaluation of temporal and spatial scaling issues in simulating soil thermal dynamics, *J Geophys Res-Atmos*, 106, 33649-33670, doi:10.1029/2001jd900151, 2001.

30

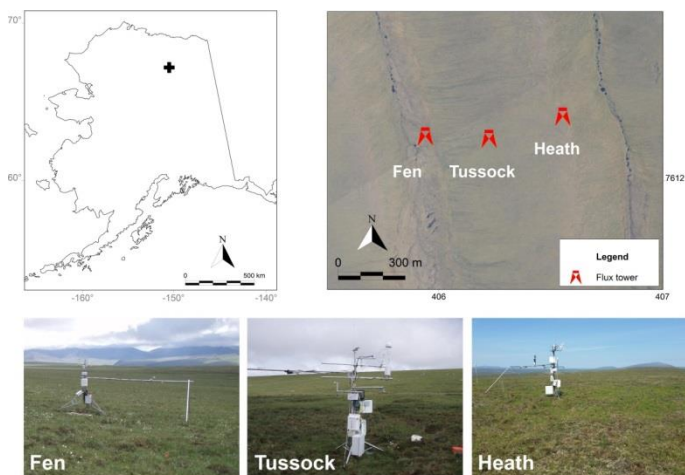


Figure 1: Location of the Fen, Tussock and Heath flux towers at Innavait watershed. Right panel map is in UTM-6N NAD83 with coordinates in km.

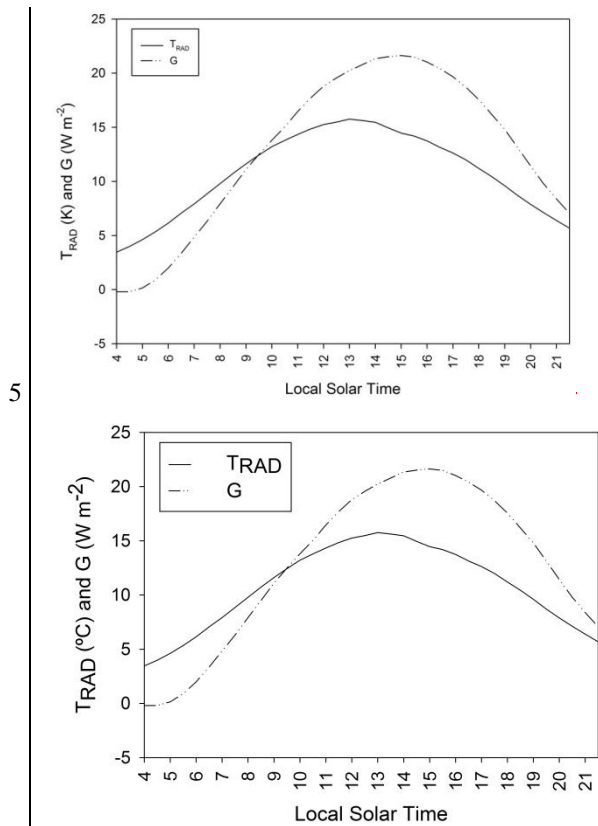


Figure 2. Mean daytime cycle for G and T_{RAD} in the study area computed using all data available from the Fen, Tussock and Heath flux towers from 2008 to 2012.

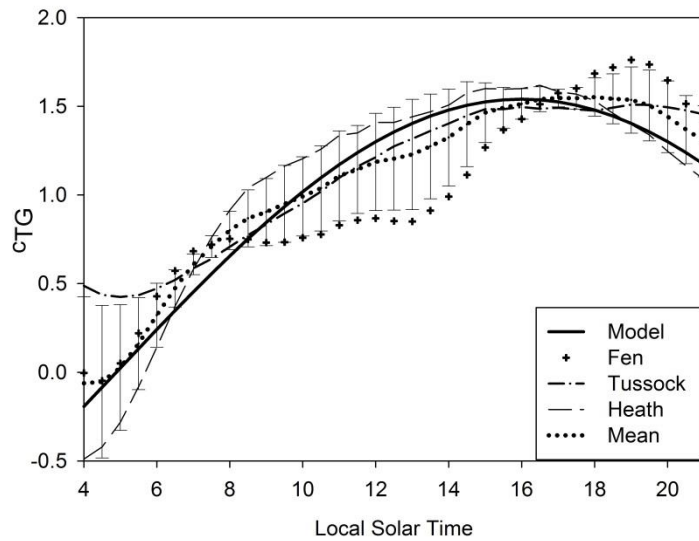
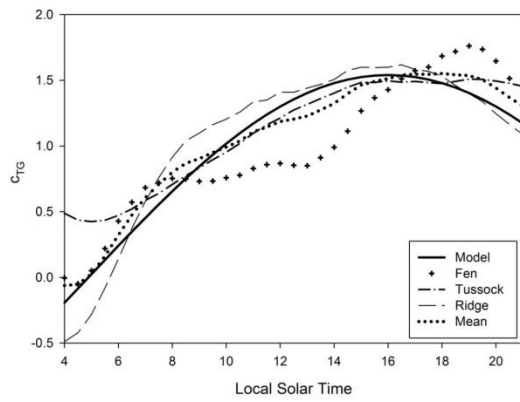
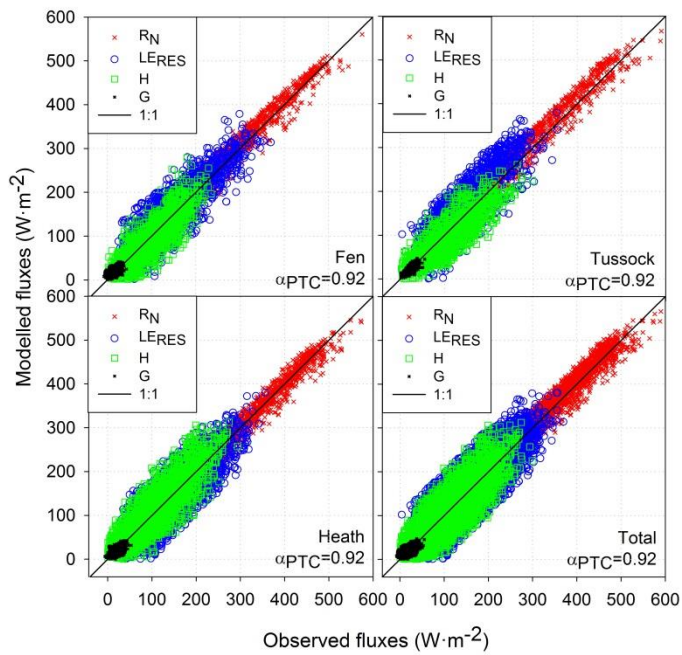
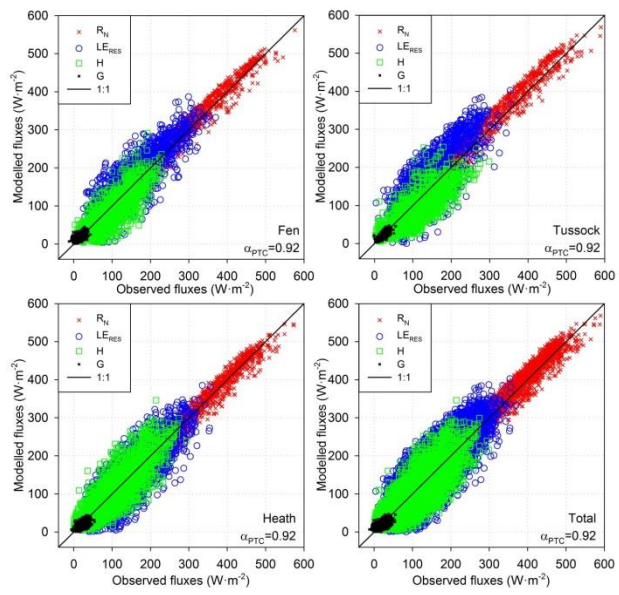
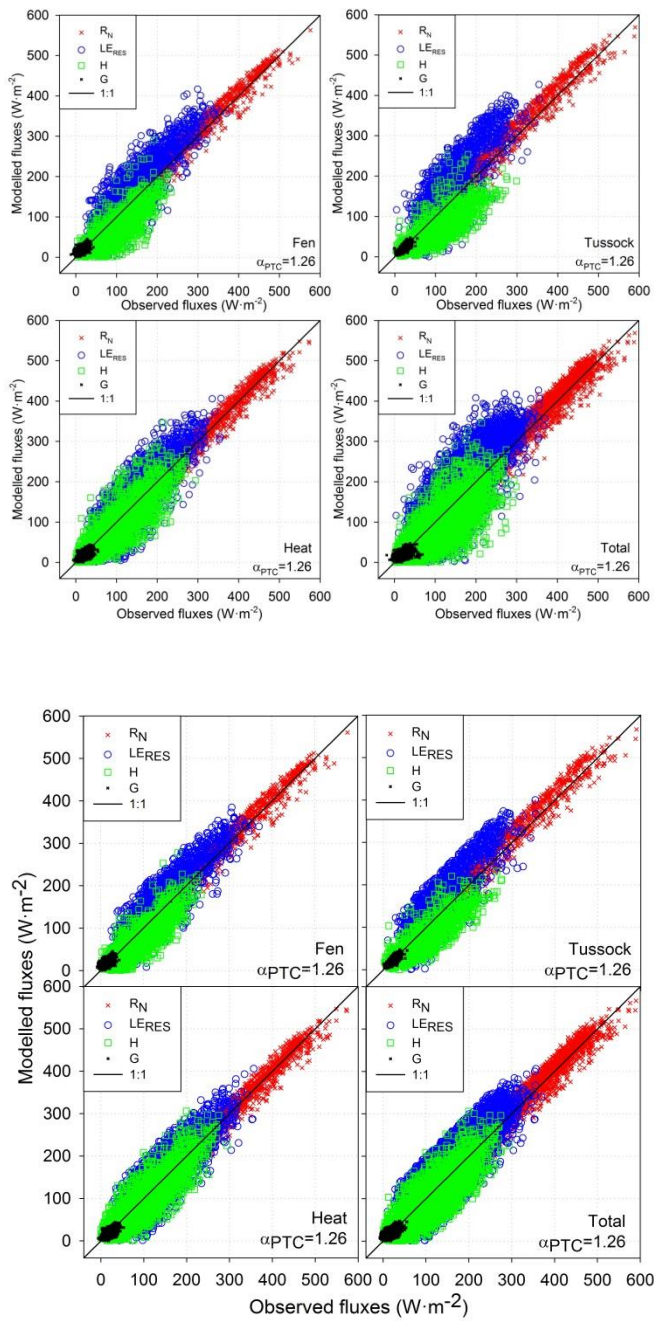


Figure 3. Time series of modeled c_{TG} and observed c_{TG} values from the Fen, Tussock and Heath flux stations as well as mean values for summer conditions. (bars represent standard deviation of the mean)



5 **Figure 4. Comparison of modeled vs. observed (using LE from residual closure) half-hourly surface fluxes using α_{PTC} of 0.92. The 1:1 line represents perfect agreement with observations.**



5 **Figure 5. Comparison of modeled vs. observed (using LE from residual closure) half-hourly surface fluxes using α_{PTC} of 1.26. The 1:1 line represents perfect agreement with observations.**

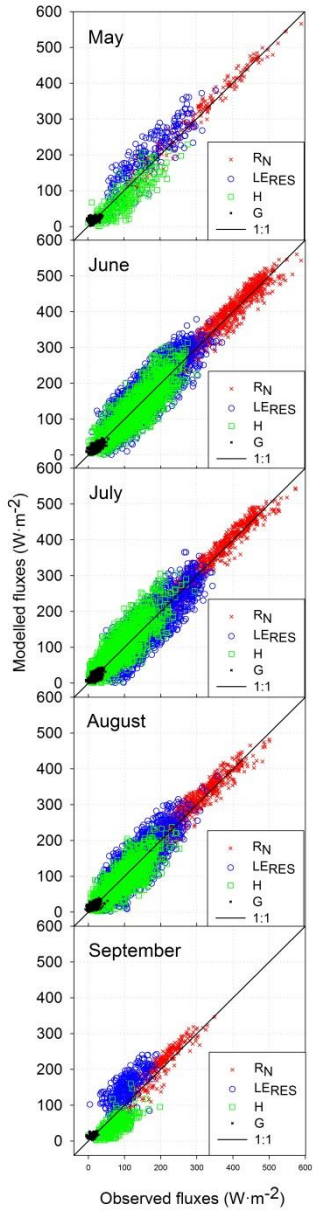
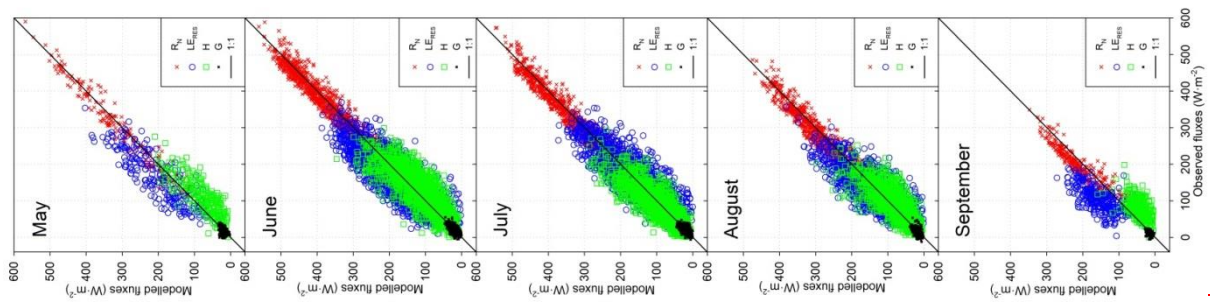
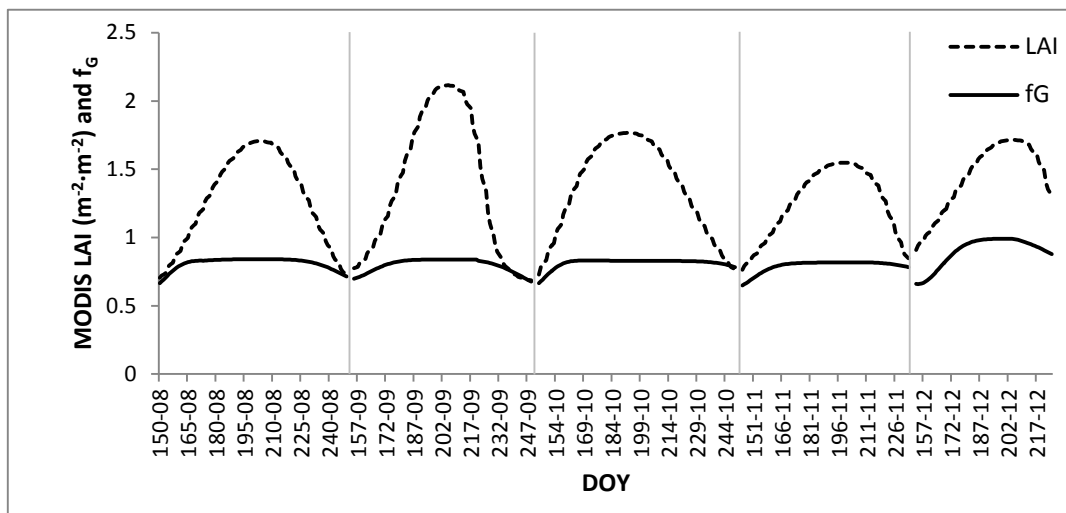
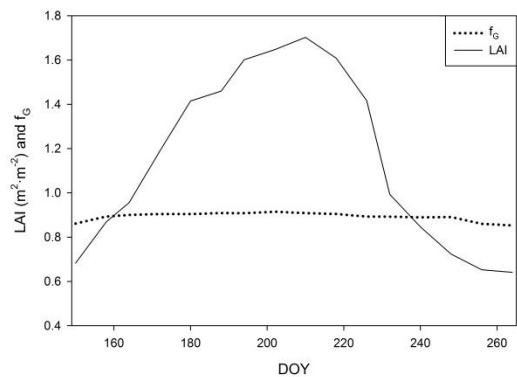
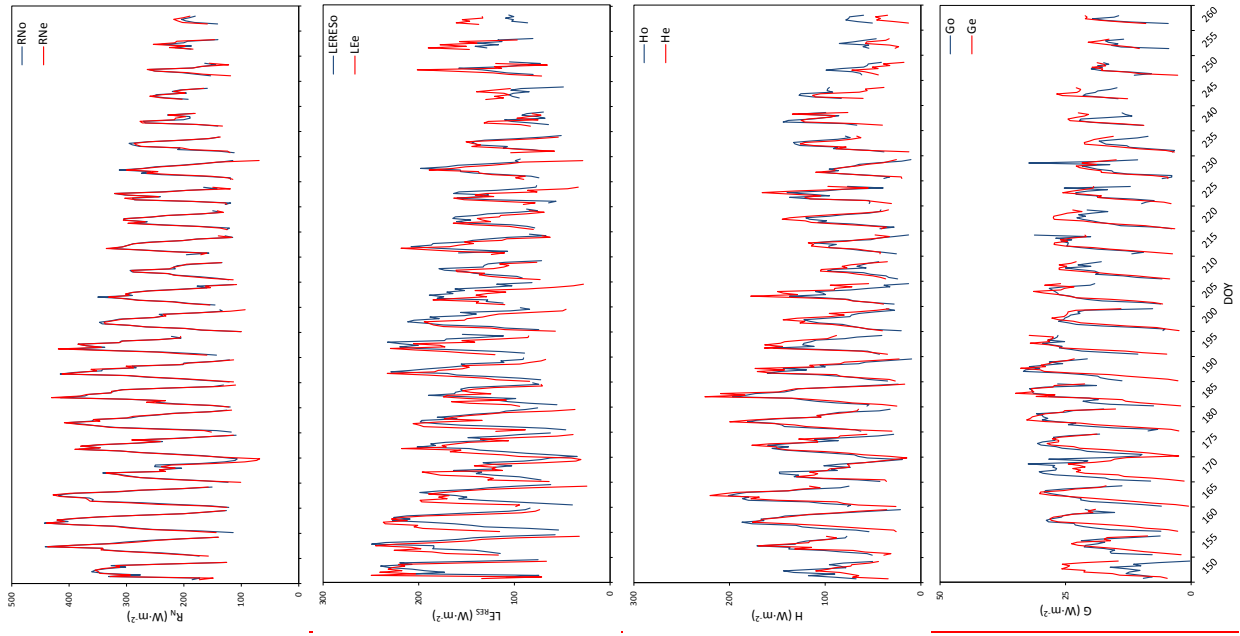


Figure 6. Comparison of modeled vs. observed (using LE from residual closure) half-hourly surface fluxes by month using α_{PTC} of 0.92 and G estimated by the new model. The 1:1 line represents perfect agreement with observations.



5 Figure 7. Mean MODIS LAI and fraction of green vegetation (f_G) temporal dynamics for all flux stations from 2008 to 2012 averaged by 8-day intervals.



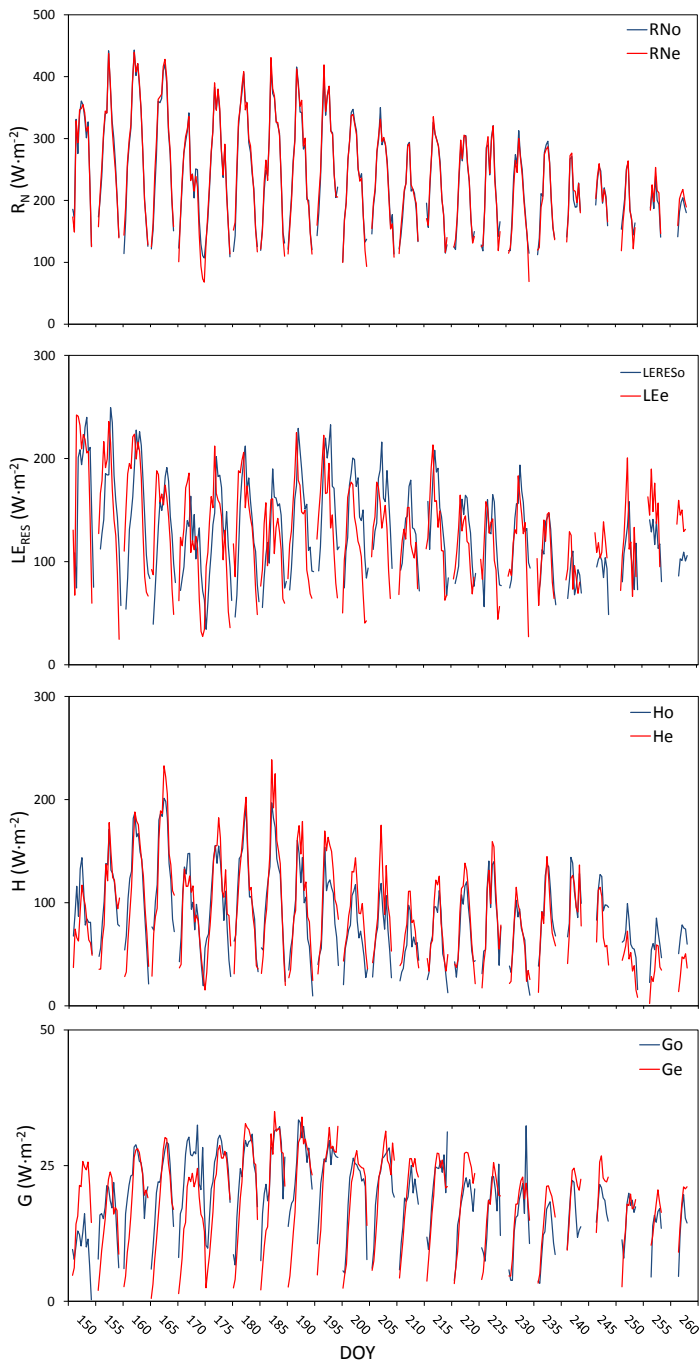


Figure 8. Comparison of hourly flux tower RN, LE, H and G observations (using LE from residual closure) (o) (from 6 to 21 hours local solar time) at the Heath flux tower with model estimates (e) using α PTC of 0.92. Each diurnal segment represents flux data averaged by hour over 5-day intervals from 2008 to 2012.

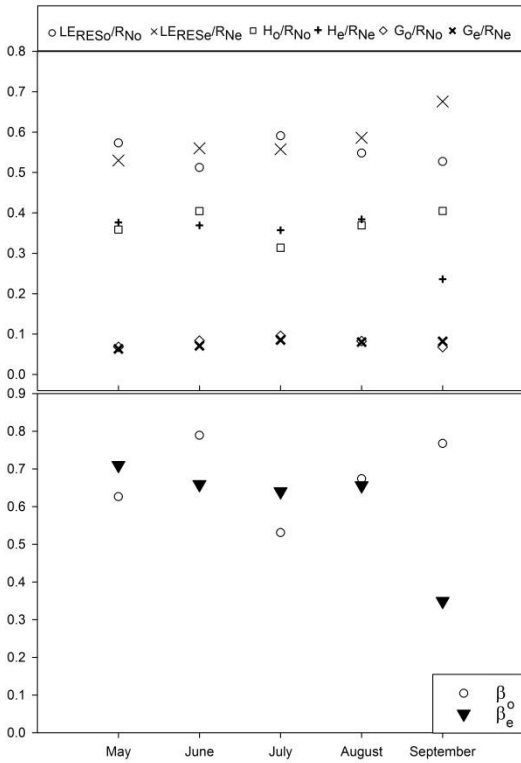
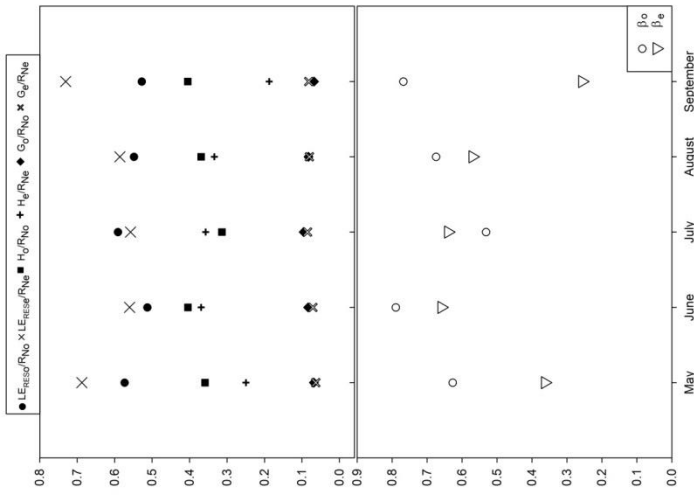


Figure 9. Monthly mean observed (o) and estimated (e) energy partitioning (LE/RN, H/RN and G/RN) and Bowen ratio (β) for all flux stations from 2008 to 2012 using α PTC of 0.92. LE observed values computed using the residual closure method.

5

10

Flux station name	Fen	Tussock	Heath
Coordinates (lat, long - WGS84)	68.606, -149.311	68.606, -149.304	68.607, -149.296
Period (Year Day of Year)	2008 194-252 2010 142-262 2011 217-262 2012 153-264	2009 194-253 2010 142-262 2012 156-226	2008 194-252 2009 159-253 2010 143-262 2011 147-262 2012 156-226
TSEB inputs	Symbol	Units	
Wind speed	u	m s^{-1}	3.3 ± 1.7
Air temperature	T_a	$^{\circ}\text{C}$	11.6 ± 3.5
Vapor pressure	e_a	kPa	0.9 ± 0.2
Atmospheric pressure	P	kPa	92 ± 0.2
Solar radiation	S_d	$\text{W}\cdot\text{m}^{-2}$	432 ± 121
Longwave incoming Longwave incoming radiation	L_d	$\text{W}\cdot\text{m}^{-2}$	261 ± 37
Surface temperature	T_s	K	288 ± 4
Leaf area index (MODIS)	LAI	$\text{m}^2\cdot\text{m}^{-2}$	1.15 ± 0.32
Canopy height	h_c	m	0.4
Clumping factor	Ω_c		1
Fraction of green vegetation	f_g		0.92 ± 0.01

Table 1. Flux station name and location, period of model evaluation and list of inputs required by the TSEB. Average and standard deviation for the input values were computed for each the full period and of model evaluation for each site.

Instrument	Description	Height/Depth(m)
Campbell Sci. CSAT3	Three Dimensional Sonic Anemometer	2.18 - 3.18
Licor LI-7500	Open Path Infrared Gas Analyzer (CO ₂ and H ₂ O)	2.18 - 3.18
Vaisalla HMP45C	Temperature and Relative Humidity Probe	1.93 - 2.82

Hukseflux HF0SCHFP01SC	Self-calibrating Soil Heat Flux PlatePlates (four per site)	0.08
Campbell Sci. TCAV	Type E Thermocouple Averaging Soil Temperature ProbeProbes (two per site)	0.02-0.04
Campbell Sci. CS616	Water Content ReflectometerReflectometers (two per site)	0.025
Licor LI190SB	PAR Sensor (incoming)	2 - 3.6
Licor LI190SB	PAR Sensor (outgoing)	2
Met One Ins. 014A	Wind Speed Sensor	1.5 - 2.26
Kipp & Zonen CMA6	Pyranometer/Albedometer	2
*Kipp & Zonen CNR4	Four components net Radiometer	2
Kipp & Zonen NR-Lite	Net radiation	2
Apogee IRR-P	InfraRed Radiometer Sensor	1.5 - 3

Table 2. General overview of the Fen, Tussock and Heath flux sites instrumentation (more information available at: <http://aon.iab.uaf.edu/innavait>). Apogee infrared radiometers were oriented 45° off-nadir at the three flux stations. Asterisk (*) means that this instrument is only available at the Tussock flux station.

	SF03							K98				
	c _G	n	R ²	RMSE	MBE	MAD	MADP	R ²	RMSE	MBE	MAD	MADP
Fen	0.30	1558	0.04	23	3	20	128	0.01	40	23	31	199
	0.14		0.04	15	-7	12	76	0.01	15	2	11	73
Tussock	0.30	1273	0.18	23	3	18	78	0.05	39	21	32	138
	0.14		0.23	17	-11	12	53	0.05	15	-4	11	46
Heath	0.30	2347	0.11	26	-5	20	96	0.10	34	14	26	125
	0.14		0.14	21	-14	15	72	0.06	16	-5	10	48
Total	0.30	5178	0.12	25	0	20	98	0.03	37	19	29	145
	0.14		0.10	18	-11	14	68	0.03	15	-3	11	53

5 Table 3. Performance statistics for the soil heat flux estimation using Santanello and Friedl (2003), SF03, and Kustas et al. (1998), K98, methodologies and two values for the maximum c_G value. RMSE, MBE and MAD are in W·m⁻² and MADP in %.

	Fit subset (60%)				Test subset (40%)				Flux subset dataset			
	Fen	Tussock	Heath	Total	Fen	Tussock	Heath	Total	Fen	Tussock	Heath	Total
R ²	0.89	0.99	0.99	0.99	0.55	0.77	0.69	0.68	0.27	0.56	0.49	0.44
RMSE	3.9	1	1	1	7	5	6	6	9	5	7	7
MBE	1.7	-0.2	-0.6	0.1	0.6	-0.3	-0.3	0	3.9	0.5	-0.3	1
MAD	2.8	1	1	1	5	4	5	4	7	4	5	6
MAPD	25	8	8	8	49	28	38	37	44	17	24	28
n	8283	10332	10748	29363	3310	4122	4273	11705	1558	1273	2347	5178

Table 4. Accuracy statistic for the new c_{TG} approach for the fit, the test and the flux subset used for Table 3 test. RMSE, MBE and MAD in W·m⁻², MADP in % and n is number of half-hour intervals.

	R _N					
	n	R ²	RMSE	MBE	MAD	MAPD
Fen	1558	0.99	23	8	18	7

Tussock	1273	0.99	25	12	19	7
Heath	2347	0.99	20	2	15	6
Total	5178	0.99	23	7	18	7

		LE _{BR}				
	n	R ²	RMSE	MBE	MAD	MAPD
Fen	1558	0.76	5345	3525	4437	4230
Tussock	1273	0.6766	5952	4333	5043	4533
Heath	2347	0.65	4943	2215	3935	3828
Total	5178	0.7071	5346	3423	4338	4235

		H				
	n	R ²	RMSE	MBE	MAD	MAPD
Fen	1558	0.66	3428	-126	2422	2523
Tussock	1273	0.65	3933	-	3426	2924
				4812		
Heath	2347	0.7271	3433	44	2726	2726
Total	5178	0.67	3532	-73	2725	2725

		LE _{RE}				
	n	R ²	RMSE	MBE	MAD	MAPD
Fen	1558	0.7574	4437	159	3329	3421
Tussock	1273	0.6968	5445	3224	4538	4026
Heath	2347	0.6768	4439	0-3	3231	3421
Total	5178	0.6869	4440	127	3532	3430

		H _{BR}				
	n	R ²	RMSE	MBE	MAD	MAPD
Fen	1558	0.6869	4739	-	3731	3927
				3224		
Tussock	1273	0.6667	5239	-	4029	3726
				3522		
Heath	2347	0.72	4538	-	3430	3425
				2414		
Total	5178	0.6869	4639	-	3631	3630
				2619		

Table 5. Accuracy and error statistics from the comparison of modelled vs. observed surface fluxes using α PTC of 0.92. n is the number of half-hour periods analysed. RMSE, MAD and MBE are in $W \cdot m^{-2}$ and MADP in %. Subscripts BR and RES are Bowen ratio and residual closure methods, respectively.

		R _N				
	n	R ²	RMSE	MBE	MAD	MAPD
Fen	1558	0.99	23	8	18	7
Tussock	1273	0.99	25	12	19	7
Heath	2347	0.99	20	2	15	6
Total	5178	0.99	23	7	18	7

		LE _{BR}				
	n	R ²	RMSE	MBE	MAD	MAPD
Fen	1558	0.73	5852	4436	4943	4735
Tussock	1273	0.6564	6356	4840	5548	4737
Heath	2347	0.6366	5548	3426	4640	4432
Total	5178	0.66	5851	3832	4843	4540

		H				
	n	R ²	RMSE	MBE	MAD	MAPD
Fen	1558	0.6462	4033	-	3226	3327
				2618		
Tussock	1273	0.5960	4639	-	3431	3229
				2924		
Heath	2347	0.67	3833	-138	3026	3026
Total	5178	0.6264	4235	-	3328	3327
				2215		

		LE _{RE}				
	n	R ²	RMSE	MBE	MAD	MAPD
Fen	1558	0.7776	4941	3020	4134	3924
Tussock	1273	0.7170	6153	4036	4745	4231
Heath	2347	0.7071	4540	169	3632	3522
Total	5178	0.7170	5344	2819	4336	4033

		H _{BR}				
	n	R ²	RMSE	MBE	MAD	MAPD
Fen	1558	0.6364	5246	-	4438	4533
				4034		
Tussock	1273	0.6062	5443	-	4335	3928
				3629		
Heath	2347	0.6765	5043	-	4035	4028
				3425		
Total	5178	0.64	5044	-	4036	4236
				3429		

Table 6. Accuracy and error statistics from the comparison of modelled vs. observed surface fluxes using α PTC of 1.26. n is the number of half-hour periods analysed. RMSE, MAD and MBE are in $W \cdot m^{-2}$ and MADP in %. Subscripts BR and RES are Bowen ratio and residual closure methods, respectively.

5

		R _N					LE				
--	--	----------------	--	--	--	--	----	--	--	--	--

	n	R ²	RMSE	MBE	MAD	MADP/MAP		R ²	RMSE	MBE	MAD	MADP/MAP	
						<u>D</u>	<u>D</u>					<u>D</u>	<u>D</u>
May	227	0.99	24	7	19	7	8	0.767	5446	3528	4538	3923	8
June	1727	0.99	22	6	17	6	0.73	4640	4911	3732	3320	3320	
July	1647	0.99	21	5	17	6	0.747	4039	-37	31	2720	2720	
August	1264	0.99	23	6	19	8	0.64	4437	407	3330	3724	3724	
September	312	0.99	26	14	23	12	0.434	5952	4539	5246	6945	4	

H						G							
	n	R ²	RMSE	MBE	MAD	MADP/MAP		R ²	RMSE	MBE	MAD	MADP/MAP	
						<u>D</u>	<u>D</u>					<u>D</u>	<u>D</u>
May	227	0.686	4236	-2922	3429	3427	9	0.12	10	1	8	48	48
June	1727	0.707	3732	-136	2925	2320	1	0.45	7	0	6	26	26
July	1647	0.72	3432	710	2425	2829		0.49	6	1	5	23	23
August	1264	0.606	3337	-87	2530	2824	2	0.40	7	3	6	34	34
September	312	0.303	4338	-3531	3732	4642	9	0.27	7	4	5	40	40

Table 7. Mean monthly accuracy and error statistics from the comparison of modelled vs. observed surface fluxes (using LE from residual closure) using α PTC of 0.92. n is the number of half-hour periods analysed. RMSE, MAD and MBE are in $W \cdot m^{-2}$ and MADP in %.